

The Takena Formation of the Lhasa terrane, southern Tibet: The record of a Late Cretaceous retroarc foreland basin

Andrew L. Leier[†]
Peter G. DeCelles
Paul Kapp

Department of Geosciences, University of Arizona, Tucson, Arizona 85721, USA

Lin Ding

Institute of Tibetan Plateau Research, Chinese Academy of Sciences, Beijing 100029, People's Republic of China

ABSTRACT

Our understanding of the processes involved in the Indo-Asian collision and the construction of the Tibetan Plateau are, in part, predicated on our understanding of the tectonic setting and crustal conditions of southern Tibet in the time period immediately preceding the Indo-Asian collision (Late Cretaceous). Several hypotheses have been proposed that describe the middle to Late Cretaceous tectonic and paleogeographic evolution of southern Tibet, each with different implications for when and how the Tibetan Plateau was uplifted. We examined the mid-upper Cretaceous Takena Formation of the Lhasa terrane in southern Tibet in order to reconstruct the middle to Late Cretaceous tectono-sedimentary history of this area and test the competing tectonic hypotheses. The Takena Formation consists of >2 km of sedimentary strata that include a lower marine limestone member (Penbo Member) and an upper member of clastic red beds (Lhunzhub Member). The Aptian-Albian Penbo Member consists of ~250 m of orbitolinid-limestone beds that were deposited in a shallow-marine seaway during a time when there was little regional subsidence. The overlying Lhunzhub Member (>1500 m) consists primarily of fluvial strata that were deposited during a period of increased subsidence. Overall, the Lhunzhub Member coarsens upward from meandering and anastomosing stream deposits interbedded with numerous paleosols near the base,

[†]Present address: Department of Geosciences, Princeton University, Princeton, New Jersey 08544, USA, aleier@princeton.edu.

to multistory-multilateral braided stream deposits near the top. The fluvial sandstone units are lithic-rich and contain abundant plagioclase and volcanic grains, and paleocurrent data record northwest-directed transport; these data indicate that the sediment was derived from the Gangdese volcanic arc that developed along the southern margin of the Lhasa terrane. Following deposition, but prior to ca. 70 Ma, the beds of the Takena Formation were folded and partially eroded. The sedimentary and stratigraphic characteristics of the Takena Formation are most consistent with deposition in a retroarc foreland basin setting. The limestone beds of the Penbo Member were deposited in a shallow-marine seaway that was eventually infilled by clastic sediment derived principally from the Gangdese volcanic arc. The low subsidence rate recorded in the lowermost strata of the Takena Formation, including the Penbo Member and the paleosol-rich interval of the Lhunzhub Member, is interpreted to be associated with the passage of a flexural forebulge. The overlying, upward-coarsening fluvial strata were deposited in progressively more proximal locations within the foredeep of a foreland basin. The Late Cretaceous folding of the Takena Formation indicates that the foreland basin strata were eventually incorporated into a fold-and-thrust belt. The upper Cretaceous sedimentary strata of the Lhasa terrane of southern Tibet predict that a north-verging fold-and-thrust belt existed along the southern margin of the Lhasa terrane during Late Cretaceous time, prior to the Indo-Asian collision. Collectively, the evidence indicates that the southern margin of the Lhasa terrane had thickened crust and was likely to have been at high elevations immediately before the Indo-Asian collision.

Keywords: Tibet, Late Cretaceous, Takena Formation, foreland basin, Lhasa, Indo-Asia collision.

INTRODUCTION

Tectonic processes play a fundamental role in shaping the physiographic features of Earth. In no other region is this more evident than in the Tibetan Plateau, which currently stands >5 km above sea level (Fig. 1; Fielding, 1996). This region serves as the archetype of continent-continent collisions, and its uplift and weathering are thought to have influenced local and global systems (e.g., Raymo et al., 1988; Raymo and Ruddiman, 1992; Molnar et al., 1993). Despite its importance, there is much about the geological history of the area that remains poorly understood.

Little is known of the crustal and topographic conditions of the Lhasa terrane of southern Tibet immediately before the Indo-Asian collision. Current hypotheses vary from those espousing thickened crust and high topography (e.g., England and Searle, 1986; Murphy et al., 1997), to those proposing that the area was characterized by thinned crust and surface elevations below sea level (e.g., Zhang, 2000). In other words, as India approached the southern margin of Asia, it is not known whether southern Tibet more closely resembled the modern Okinawa Trough or the modern Bolivian Andes.

Three models have been proposed to explain the mid-Late Cretaceous tectonic evolution of the Lhasa terrane of southern Tibet (Fig. 2). Beginning in the Early Cretaceous, Neotethyan oceanic crust was consumed in a north-dipping subduction zone along the southern margin of Eurasia, which ultimately led to the formation of the Gangdese magmatic arc (e.g., Tapponnier et al., 1981; Burg and Chen, 1984; Allégre et al.,

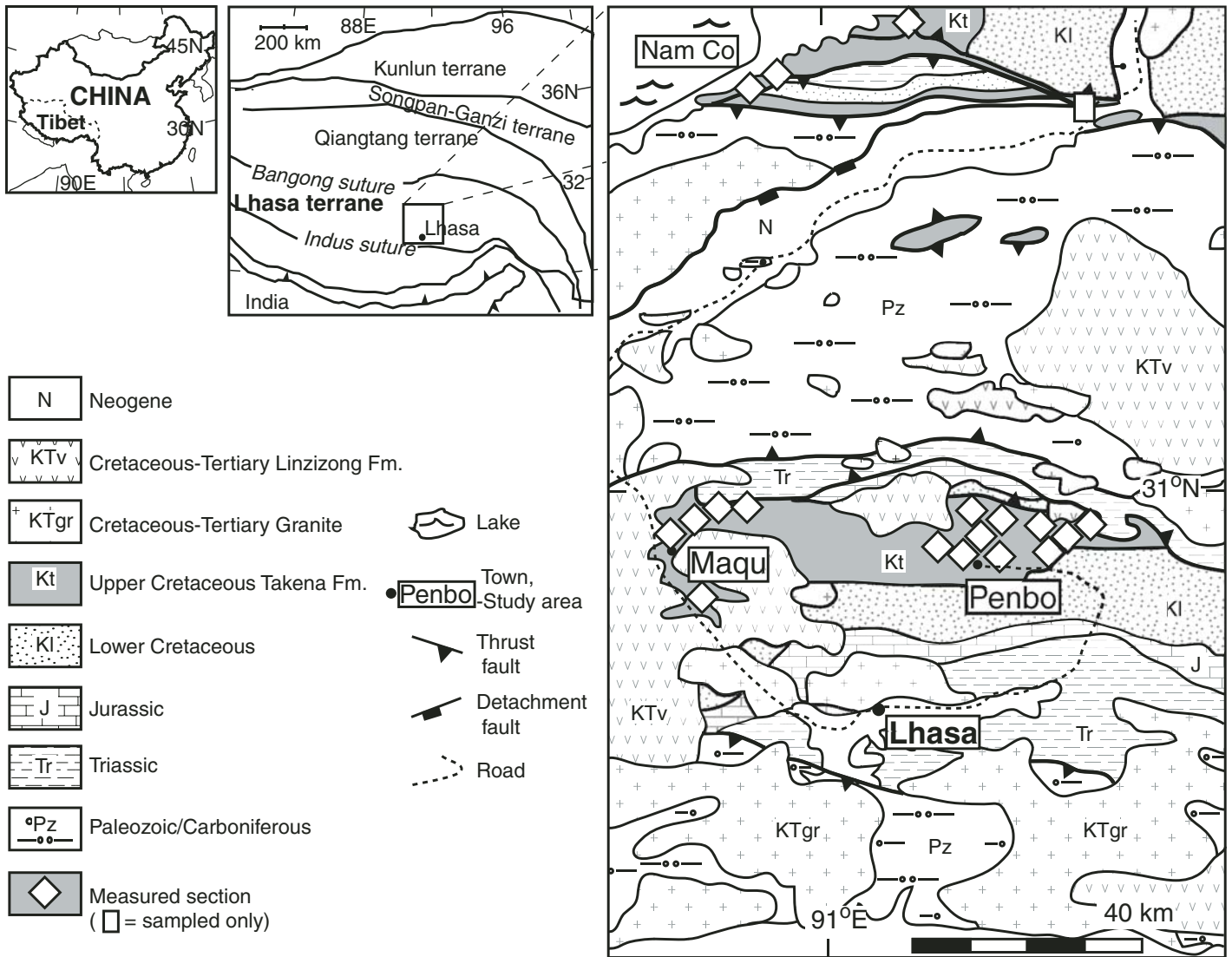


Figure 1. Location map and geology of the study area (geology modified from Liu, 1988). The Lhasa terrane is the southernmost of several terranes that compose the Tibetan Plateau. The study area includes the territory between the city of Lhasa and the lake Nam Co. Sections were measured in three principal locations: Penbo, Maqu, and Nam Co.

1984). Thus, this area is often postulated as having been an “Andean-style” convergent margin during the mid–Late Cretaceous (e.g., Allégre et al., 1984; England and Searle, 1986; Ratschbacher et al., 1993; Chen et al., 1993; Fielding, 1996; Burg et al., 1983). But how “Andean” was this margin? The retroarc region in the Andes has a well-developed fold-and-thrust belt, crustal thicknesses in excess of 70 km, and surface elevations >6 km above sea level (e.g., Beck and Zandt, 2002). With the exception of locally folded Cretaceous strata, evidence supporting this hypothesis is relatively sparse. Existing paleocurrent data from Late Cretaceous rocks indicate that sediment was derived from northern Lhasa (Leider et al., 1988), which is

contrary to what is predicted in the retroarc foreland basin model. Furthermore, not all retroarc regions experience shortening. The second proposed model suggests that the Lhasa terrane was occupied by a backarc extensional basin, which was located atop thinned continental crust (Zhang, 2000). Alternatively, the third tectonic model hypothesizes that the defining tectonic event within the Lhasa terrane during this time may have had little to do with subduction of Neotethyan oceanic crust. This last model postulates that tectonism in southern Tibet was dominated by the Late Jurassic–Cretaceous collision of the Lhasa terrane with the southern margin of Asia. The resulting uplift and crustal loading along the accretionary suture should

have produced a peripheral foreland basin in the Lhasa terrane (Leider et al., 1988; Dürr, 1996; Murphy et al., 1997).

The sedimentary record of the ~2-km-thick middle to Late Cretaceous Takena Formation can be used to test the aforementioned tectonic models. In this paper we present: (1) detailed descriptions of the lithologies, petrography, facies, and regional architecture of the Takena Formation in southern Tibet; (2) reconstructions of sediment sources, transport directions, and depositional histories of the Late Cretaceous sediment; (3) interpretations of Cretaceous paleogeographies and basin development; and (4) an interpretation of the Late Cretaceous tectonic setting of the southern Lhasa terrane that is

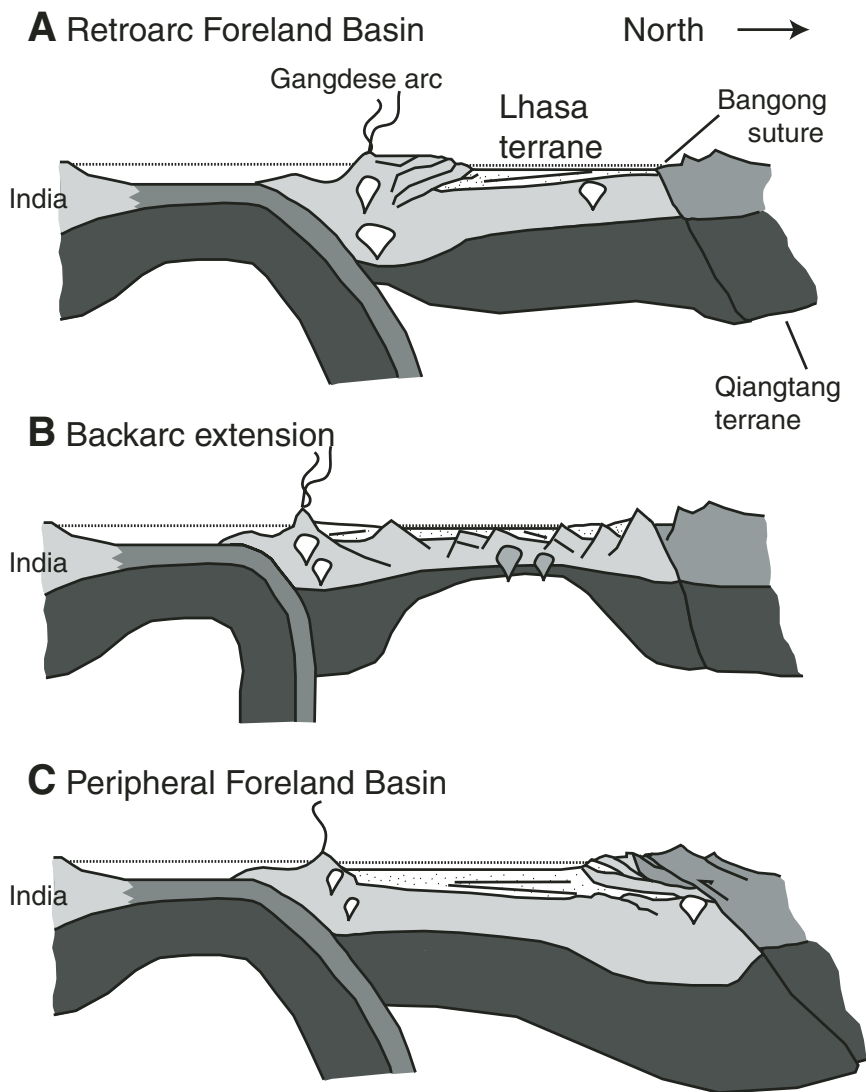


Figure 2. Proposed tectonic models. (A) The Takena Formation may have been deposited in a retroarc foreland basin that developed on the northern side of the Gangdese magmatic arc (e.g., England and Searle, 1986). (B) Accommodation for the Takena Formation may have been caused by backarc extension, possibly associated with southward rollback of Neotethyan oceanic crust (e.g., Zhang, 2000). (C) The Cretaceous tectonic setting may have been largely controlled by deformation that resulted from the Late Jurassic–Early Cretaceous collision between the Lhasa terrane and the Qiangtang terrane to its north (e.g., Leeder et al., 1988). Not to scale.

consistent with both sedimentological and structural data. Our results are based on more than 5500 m of detailed measured stratigraphic sections, 593 paleocurrent measurements gathered at 36 locations, new biostratigraphic constraints, and petrographic data from 42 thin sections, augmented with clast counts. Collectively, the data indicate that the upper Cretaceous Takena Formation was deposited in a retroarc foreland basin, which formed to the north of a Cretaceous fold-and-thrust belt.

REGIONAL GEOLOGY

Stratigraphy and Age Control

The Takena Formation is exposed in the Lhasa terrane of southern Tibet (Fig. 1). It overlies Early Cretaceous marginal-marine strata and is in turn unconformably overlain by Late Cretaceous–early Tertiary volcanic strata of the Linzizong Formation (Fig. 3; Yin et al., 1988). In the southern half of the study area (Penbo

and Maqu areas; Fig. 1), the Takena Formation consists of a basal limestone member (Penbo Member) and an overlying succession of fluvial red beds (the Lhunzhub Member; Fig. 3; Yin et al., 1988). Fossils indicate that these limestone beds were deposited during Aptian through late Albian time. The fossil assemblages include: echinoids *Macraster* and *Salenia*, ammonoids of the family Parahoplitidae, most similar to *Kazanskyella fosteri* or *K. cuchillensis*, and foraminifera *Orbitolina* (*Mesorbitolina*) *texana* Roemer (R.W. Scott, 2004, personal commun.). In the northern half of the study area, the Cretaceous limestone thickens and biostratigraphic evidence indicates that it was deposited over a longer duration (Barremian–Cenomanian; Smith and Xu, 1988; Zhang et al., 2004; this study). This thicker limestone unit is called the Langshan Formation (Yin et al., 1988; Leeder et al., 1988). Therefore, the Takena Formation in the northern portion of the study area consists only of fluvial red beds; however, the general lithologic progression from lower carbonate to upper clastic red beds remains the same. The depositional age of the terrestrial clastic section overlying the basal limestone is poorly constrained, although Smith and Xu (1988) reported a Cenomanian bivalve from a carbonate bed within the succession. The youngest U–Pb ages of detrital zircons collected from fluvial sandstone cluster at 105 ± 2 Ma, providing a maximum depositional age for the upper part of the Takena Formation (Leier et al., 2004). The minimum depositional age is constrained by U–Pb zircon ages of 69 ± 2.4 Ma from volcanic strata within the overlying Linzizong Formation (He, 2005). A 90 Ma igneous dike cuts across unspecified beds of the Takena Formation (Coulon et al., 1986), so that although unambiguous constraints restrict deposition of the fluvial Lhunzhub Member of the Takena Formation to ca. 105–70 Ma, we infer that nonmarine deposition began in roughly late Albian time (ca. 105–100 Ma) and most likely ended in Turonian time (ca. 90 Ma).

Tectonic History

The Lhasa terrane was the last of a series of continental fragments to accrete onto southern Asia during the Phanerozoic before the collision with India (Allégre et al., 1984; Dewey et al., 1988; Yin and Harrison, 2000). Rifting from Gondwanaland during the Late Permian–Early Triassic, the Lhasa terrane moved northward as Mesotethyan oceanic crust north of the Lhasa terrane was subducted northward beneath the Qiangtang terrane (e.g., Allégre et al., 1984; Dewey et al., 1988; Şengör and Natal'in, 1996). The northern boundary of the Lhasa terrane is the Bangong suture, which

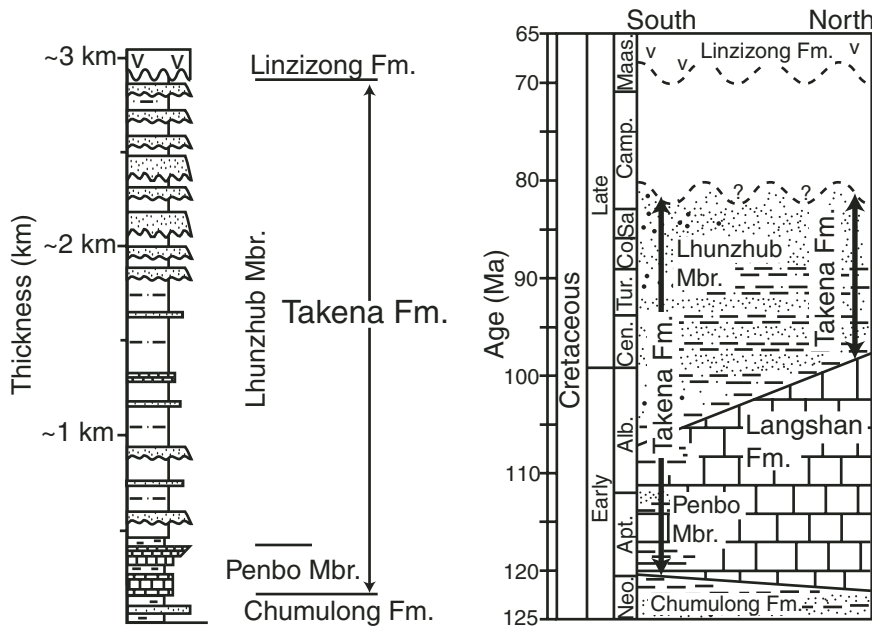


Figure 3. Generalized Cretaceous stratigraphy. The Takena Formation consists of a basal limestone member, but is primarily composed of clastic red beds belonging to the Lhunzhub Member. From south to north, Aptian-Albian limestone increases in thickness and was deposited over a greater time span. Figure has been modified from Yin et al. (1988).

formed as a result of the collision between the Lhasa and Qiangtang terranes during the Late Jurassic–Early Cretaceous (Fig. 1; Dewey et al., 1988; Yin and Harrison, 2000). Along the southern margin of the Lhasa terrane, Cretaceous–Paleogene subduction of Neotethyan oceanic crust produced the Cretaceous–Tertiary Gangdese magmatic arc (e.g., Allégre et al., 1984; Coulon, et al., 1986). The Indus–Yarlung suture marks the southern boundary of the Lhasa terrane and formed as a result of the Indo–Asian collision, which occurred between 70 and 38 Ma (see Butler, 1995; Yin and Harrison, 2000). The exact timing of the collision is still in dispute; however the majority of estimates suggest that contact between Indian and Asian continental crust occurred ca. 55 Ma (for a more thorough review, see Guillot et al., 2003, and Leech et al., 2005). During deposition of the Takena Formation, paleomagnetic data place the Lhasa terrane at roughly 10°N latitude (Achache and Courtillot, 1984; Besse and Courtillot, 1988; Chen et al., 1993).

SEDIMENTOLOGY OF THE TAKENA FORMATION

Lithofacies

Lithofacies within the Takena Formation are typical of carbonate and clastic rocks, and are

well understood in terms of depositional processes. Individual lithofacies are described and interpreted in Table 1. The following paragraphs focus on genetic associations of lithofacies that can be more broadly interpreted in terms of depositional systems.

Lithofacies Associations

Depositional environments of the Takena Formation were interpreted from 18 detailed stratigraphic sections measured in the Penbo, Maqu, and Nam Co areas (Fig. 1). A composite stratigraphic section of the Takena Formation is shown in Figures 4–6. The individual lithofacies are grouped into six lithofacies associations: (1) a basal marine limestone lithofacies association (between ~50 and 250 m in Fig. 5); (2) a marginal-marine siltstone lithofacies association (between ~250 and 300 m in Fig. 5); (3) a lower fluvial lithofacies association (between ~300 and 1200 m in Fig. 5); (4) a middle limestone lithofacies association (between ~0 and 50 m in Fig. 6); (5) a middle siltstone lithofacies association (between ~50 and 800 m in Fig. 6); and (6) an upper fluvial lithofacies association (between ~800 and 1100 m in Fig. 6). These lithofacies associations are presented in the order of their stratigraphic position within the Takena Formation, beginning with the lowermost unit (Figs. 5 and 6).

Lower Marine Limestone Lithofacies Association—Description

In the southern portion of the study area, the lowest part of the Takena Formation consists of orbitolinid-bearing limestone and lesser amounts of clastic siltstone (lithofacies C1, F3; Table 1). These lithologies comprise the Penbo Member and conformably overlie lower Cretaceous marginal-marine siltstone and sandstone (between ~0–50 m in Fig. 5). The lowermost limestone of the Takena Formation is a wackestone that contains fossils of orbitolinids (*Mesorbitolina* sp.), echinoids (*Macraster* sp., *Selina* sp.), and rare oysters (*Ceratosreon*?) and ammonites (*Kazanskyella* sp.) (R.W. Scott, 2004, personal commun.). Overlying these wackestone beds are a series of ~3-m-thick limestone cycles composed, from base to top, of marly siltstone, orbitolinid-wackestone (*Mesorbitolina texana* [Roemer]; R.W. Scott, 2004, personal commun.), and fossiliferous orbitolinid packstone, which also contains echinoderm debris, rare ostracodes, and disarticulated bivalves (Fig. 7). The packstone beds at the top of each cycle have sharp upper surfaces and are overlain by marly siltstone of the overlying cycle. Individual cycles can be correlated between sections that are >10 km apart. In the Maqu area (Fig. 1), the lower orbitolinid-bearing limestone lacks obvious cycles but is otherwise similar to the limestone in the Penbo region. Limestone beds in the Nam Co region are poorly exposed but consist of laminated to massive peloidal mudstone (lithofacies C3). Rudist boundstones of Aptian–Albian age have been described elsewhere in the Lhasa terrane (Leeder et al., 1988; Leier, 2005). Laminated green siltstone beds and local very fine-grained sandstone beds with oscillatory current ripples are present in minor amounts within this lithofacies association in the Maqu and Penbo locations (lithofacies F3).

Lower Marine Limestone Lithofacies Association—Interpretation

The basal marine limestone lithofacies association records deposition in a low-energy, carbonate-dominated, shallow-water marine environment. The lowermost wackestone in the Penbo area, the peloidal mudstone in the Nam Co area, and the wackestone in the Maqu area, are interpreted to have been deposited in quiet, muddy, lagoonal environments (e.g., Leeder et al., 1988; Tucker and Wright, 1990; Jones and Desrochers, 1992). Based on the presence of rudist boundstone elsewhere in the region, these strata were likely deposited in shallow-marine lagoons that were situated between rudist patch reefs (e.g., Leeder et al., 1988; Leier, 2005). The carbonate cycles are interpreted as carbonate parasequences that record repeated shoaling and flooding in a

TABLE 1. LITHOFACIES

Description	Interpretation
G1. Imbricated conglomerate Clast-supported pebble conglomerate; rare cobbles; imbricated clasts; sandy matrix; crude horizontal stratification; erosional base	Deposits associated with traction transport by high-competency water flows
S1. Trough cross-stratified sandstone Fine- to very coarse-grained trough cross-stratified sandstone (sets typically <1m); occasionally with pebbles and granules	Deposits of migrating, subaqueous, three-dimensional sand dunes
S2. Plane-parallel laminated sandstone Horizontal beds of fine- to coarse-grained, well-sorted sandstone; plane-parallel laminations	Subaqueous deposits associated with upper-flow regime conditions
S3. Large, planar cross-stratified sandstone Fine- to medium-grained; large (>1 m thick) relatively low-angle (~20°) planar to slightly trough-shaped cross-stratification; bases are slightly erosional	Deposits of large, migrating, subaqueous, two- to three-dimensional transverse dunes or bars
S4. Sandstone with asymmetric ripples Very fine- to medium-grained; asymmetric ripples and ripple cross-lamination; beds < 5 cm thick; occasional sub- and supercritical climbing ripples	Deposits of migrating subaqueous ripples under a unidirectional current; climbing ripples deposited under high sedimentation rates
S5. Sandstone with symmetric ripples Very fine- to fine-grained; symmetrical ripple laminae; muddy laminae occasionally interbedded	Deposits of ripples formed in oscillating currents; muddy laminae suggest alternating energy levels
S6. Massive sandstone Very fine- to coarse-grained; structureless; occasional faint laminae and burrows	Deposits of sandy gravity flows or original sedimentary structures destroyed by bioturbation
F1. Massive red mudstone No sedimentary structures; commonly red to purple and mottled; CaCO ₃ nodules; occasional root traces and vertical burrows (~3 cm diameter)	Paleosols formed in a relatively well-drained environment
F2. Red siltstone Siltstone, primarily red, with rare laminations and asymmetric ripples; does not contain CaCO ₃ nodules; interbedded with very fine- and fine-grained sandstone; locally interbedded with thin ostracode-bearing beds	Deposits of a low-energy environment, either terrestrial or shallow marine; red color suggests oxidized nonmarine setting
F3. Green laminated siltstone Laminate green siltstone, commonly with marine fossils; occasionally marly; local thin beds of very fine-grained sandstone	Deposits of a low-energy, clastic, shallow-marine environment
C1. Orbitolinid packstone and wackestone Laterally continuous beds with orbitolinid tests; rare bivalve and echinoid fragments	Deposits associated with a low-energy shallow-marine environment
C2. Oyster wackestone and packstone Wackestone and packstone composed almost entirely of disarticulated oyster shells	Shallow-marine deposits, possibly estuarine/lagoonal setting
C3. Pelloidal mudstone Massive; micritic; rare laminations	Deposits of a low-energy shallow-marine environment

Measured sections

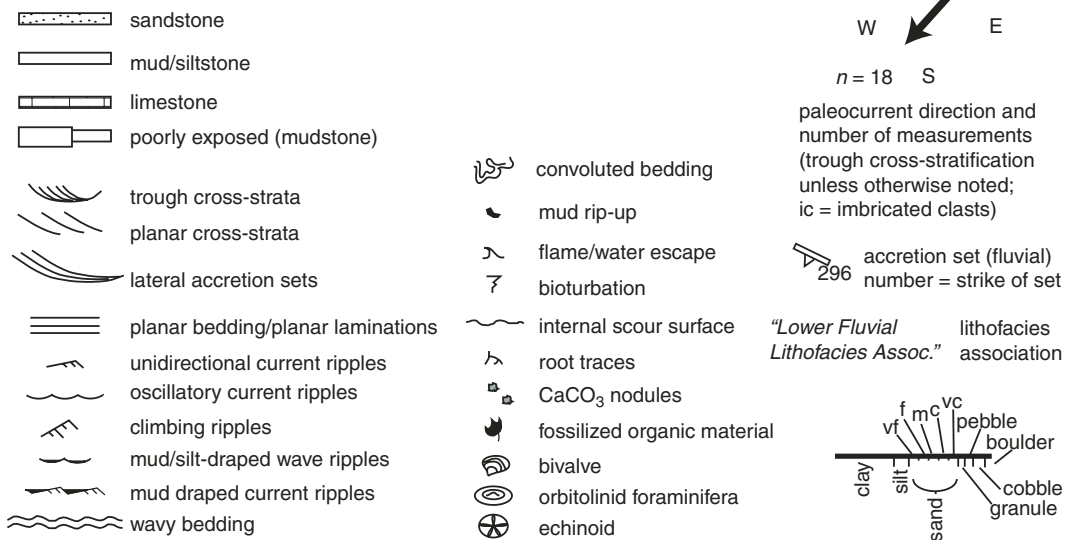


Figure 4. Stratigraphic symbols: Key to symbols used in the stratigraphic sections in Figures 5 and 6.

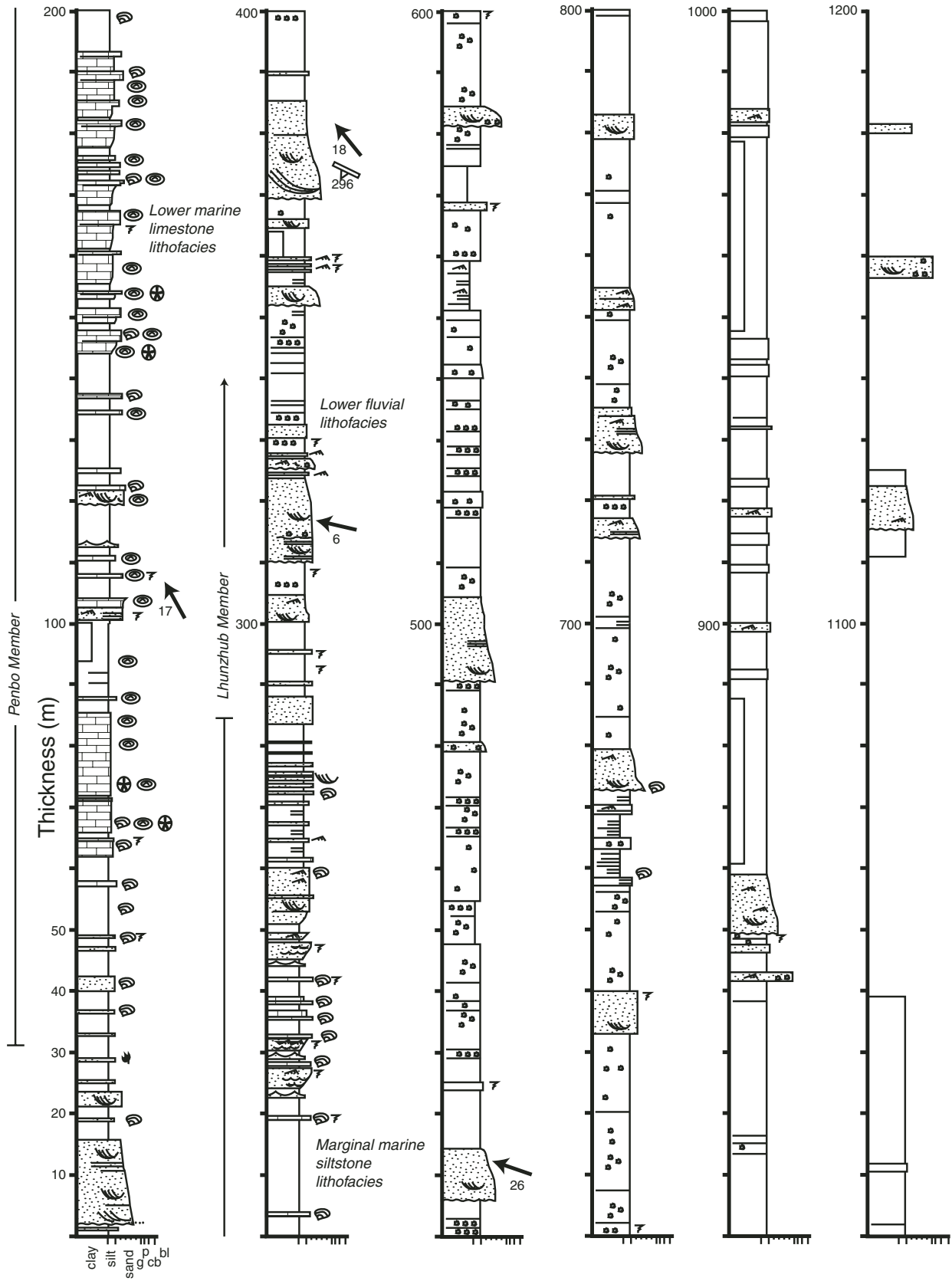


Figure 5. The lower part of the Tadena Formation in the Penbo area. The Tadena Formation contains a basal succession of limestone (~50–250 m), which is conformably overlain by clastic strata of the Lhunzhub Member. The base of the Lhunzhub Member contains numerous paleosols. See also Figures 7, 8, and 9.

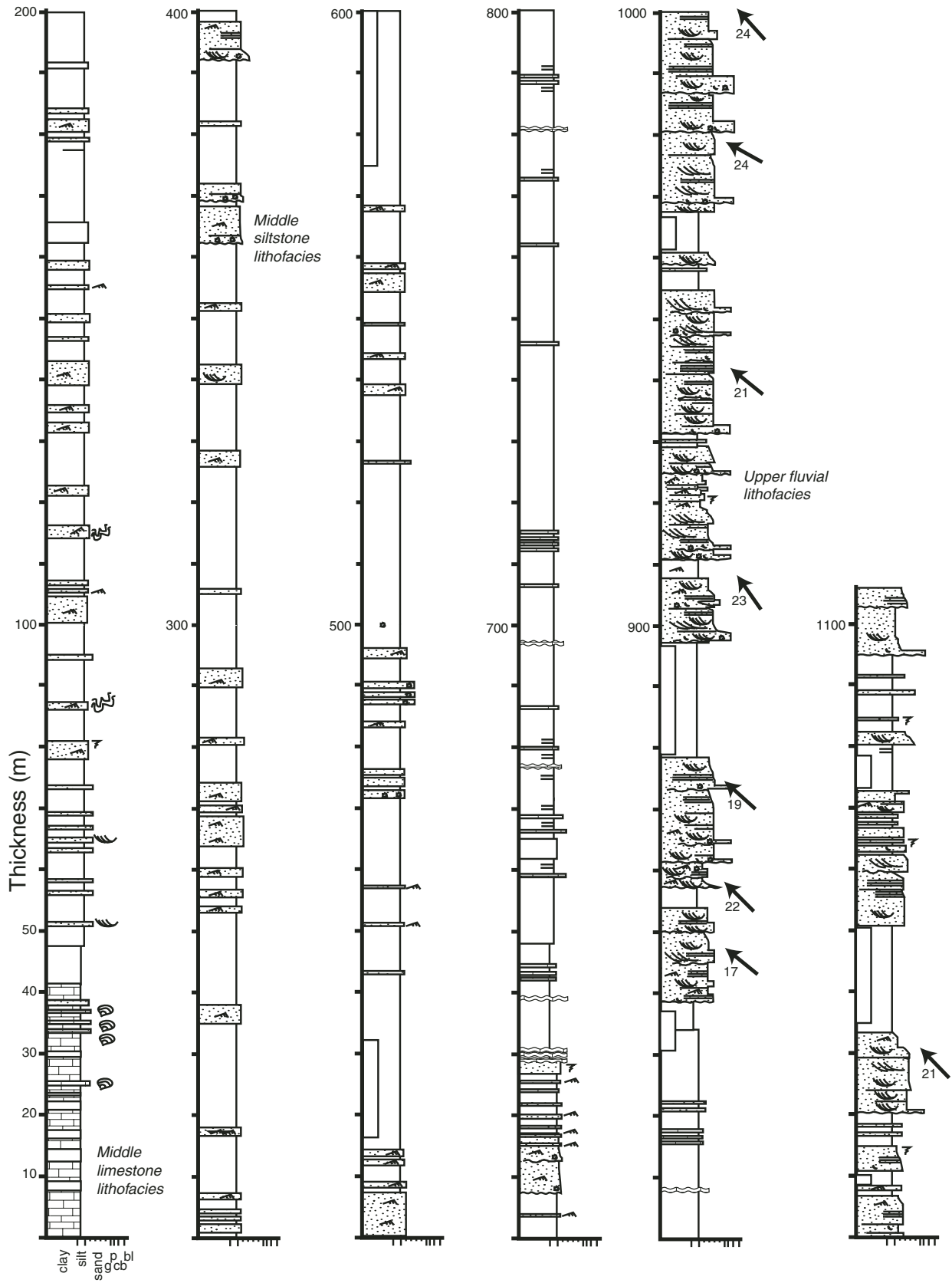


Figure 6. The upper part of the Takena Formation in the Penbo area. A thin oyster-bearing limestone unit is overlain by a thick succession of relatively fine-grained strata, which coarsen upward and contain thick sandstone sequences. Note that the contact between the lower (Fig. 5) and upper (this figure) part of the Takena Formation is not exposed. See also Figure 10.

shallow-marine environment (e.g., Inden and Moore, 1983; Jones and Desrochers, 1992). The presence of siltstone within this lithofacies association in the Penbo and Maqu areas suggests that although these areas were characterized by carbonate sedimentation, they also received occasional influxes of fine-grained clastic material.

Marginal-Marine Siltstone Lithofacies

Association—Description

The marginal-marine siltstone lithofacies association conformably overlies the lower marine limestone lithofacies association (Fig. 5). This lithofacies association consists of green siltstone and interbedded very fine-grained sandstone (lithofacies F3). Both the siltstone and sandstone contain marine fossils, including disarticulated bivalves and rare ammonites (*Kazanskyella—fosteri* or *cuchillensis*; R.W. Scott, 2004, personal commun.). Siltstone intervals commonly grade into sandstone beds. Beds of sandstone typically contain oscillatory and unidirectional current ripples, wavy-bedding, mud-draped oscillatory current ripples, and subvertical and subhorizontal burrows (lithofacies S5). Locally, stacked beds of sandstone coarsen upward from very fine-grained to fine-grained.

Marginal-Marine Siltstone Lithofacies

Association—Interpretation

Strata of the marginal-marine siltstone lithofacies association were deposited in a low-energy, shallow-marine environment. The upward-coarsening siltstone and sandstone sequences containing oscillatory current ripples and mud-draped ripples are interpreted as deposits of prograding, low-energy shorelines or tidal flats (e.g., Walker and Harms, 1971; Elliot, 1974; Reinson, 1992). Deposits with similar characteristics can be associated with deeper-water offshore environments; however, a shallow-water interpretation is preferred because this lithofacies association grades conformably into overlying terrestrial deposits (Fig. 5; see following).

Lower Fluvial Lithofacies Association—

Description

The marine siltstone lithofacies association grades into red mudstone, sandstone, and local conglomerate that comprise the lower fluvial lithofacies association (Fig. 5). Strata of the lower fluvial lithofacies association are characterized by ~10-m-thick sandstone units interstratified with mottled, red, CaCO₃ nodule-bearing mudstone (Fig. 8). Two types of sandstone units occur within the lower fluvial succession, which are designated type-A and type-B sandstone units. The lower fluvial lithofacies association in the Penbo area consists largely of the type-A sandstone units, whereas the Maqu and

Nam Co areas have both type-A and type-B sandstone units.

The type-A sandstone units overlie a basal scour surface, are generally <10 m thick, and in their lowest portions have medium-grained sandstone beds with abundant mudstone intraclasts. Sandstone in the lower two-thirds of the units is trough cross-stratified, whereas in the upper third the sandstone contains plane-parallel laminations and unidirectional current ripples (lithofacies S1, S2, S4). Large-scale cross-bedding (>2 m amplitude) that dips in directions perpendicular to the paleocurrent direction (as measured by trough cross-stratification; see following) occurs in a few sandstone units (Fig. 5). As a whole, the sandstone units fine upward continuously and lack prominent internal scour surfaces or abrupt changes in grain size (Fig. 5). Sandstone beds at the top of a sequence are typically massive or bioturbated and grade into overlying red siltstone (lithofacies S6).

Type-B sandstone units (~10 m thick) overlie basal scour surfaces and are composed of two or more ~2–4-m-thick sandstone packages separated from one another by scour surfaces. Individual packages tend to be laterally discontinuous, typically fine upward, and contain trough cross-stratification as well as occasional large, planar cross-stratification (~1 m amplitude; lithofacies S1, S3). Plane-parallel laminations and rare current ripples are present in the upper ~0.5 m of many packages, but these features are often partially eroded by the basal scour of the overlying sandstone package. Although the constituent sandstone packages may fine upward slightly, the grain size of the sandstone sequence as a whole remains relatively constant from base to top. In some locations in the Maqu area, these units also contain beds of pebble-conglomerate (lithofacies G1). Normally, the contact between the uppermost sandstone and the overlying siltstone is sharp.

The mudstone and siltstone beds between both type-A and type-B sandstone units are typically mottled and contain CaCO₃ nodules and rare root traces (Fig. 8; lithofacies F1). Interbedded with the mudstone is thinly bedded, fine-grained sandstone that contains unidirectional current ripples, climbing ripples, and subvertical burrows.

Lower Fluvial Lithofacies Association—

Interpretation

The grain-size trend, facies, and architecture of type-A sandstone units are typical of sandy meandering river deposits (e.g., Allen, 1964; Miall, 1996). The large-scale cross-bedding is interpreted as accretion sets (Allen, 1964); their orientation relative to paleocurrent direction indicates lateral migration of the paleochannel.

The upward-fining trend within the sandstone units and the corresponding change from subaqueous dune trough cross-stratification to ripple cross-stratification (lithofacies S1, S4) reflect a progressive decrease in flow strength as the river channel was infilled and migrated laterally across the floodplain (e.g., Allen, 2001).

The architectural elements, grain-size trend, and internal facies of the type-B sandstone units are most consistent with deposition by low-sinuosity, sandy braided rivers (Cant and Walker, 1978; Miall, 1978; Willis, 1993a; Miall, 1996). Multilateral and multistory sandstone units are most often associated with unstable channels like those in sandy braided streams (Miall, 1996). Trough cross-stratified sandstone was deposited by subaqueous 3-dimensional (3-D) dunes that migrated within the paleochannels. The sandstone beds with relatively larger and more planar cross-stratification are interpreted as deposits of migrating 2-dimensional (2-D) dunes or transverse bars. The plane-parallel laminated sandstone near the top of individual packages is interpreted as having been deposited within either infilled channels or on bar-tops where flow depth was shallow; local siltstone beds deposited atop plane-parallel laminated sandstone are interpreted as having been deposited during the waning stages of flow (e.g., Langford and Bracken, 1987; Bristow, 1993). Multiple internal scour surfaces within sandstone units indicate periods of channel reoccupation or episodic increases in flow strength.

Mudstone intervals within the lower fluvial lithofacies association are interpreted as overbank sediments deposited in floodplain environments that were located adjacent to fluvial channels (Allen, 1964). The rippled, fine-grained sandstone beds record periodic crevasse splay events. Mottled mudstones that lack primary sedimentary structures and contain CaCO₃ nodules are interpreted as paleosols that formed on relatively well-drained portions of the floodplain (Calcisol, *sensu* Mack et al., 1993). Paleosols are abundant within this lithofacies association; in some instances, four or more paleosols are stacked atop one another (Fig. 8), suggesting periods with relatively low sedimentation rates (e.g., Kraus, 1999).

Middle Limestone Lithofacies Association—

Description

The middle limestone lithofacies association consists of an ~50-m-thick limestone interval that overlies the lower fluvial lithofacies association in the Penbo and Maqu localities (Fig. 6); this portion of the Takena Formation is not exposed in the Nam Co area. The limestone consists of oyster-bearing packstone and wackestone beds (<0.5 m thick) interbedded with

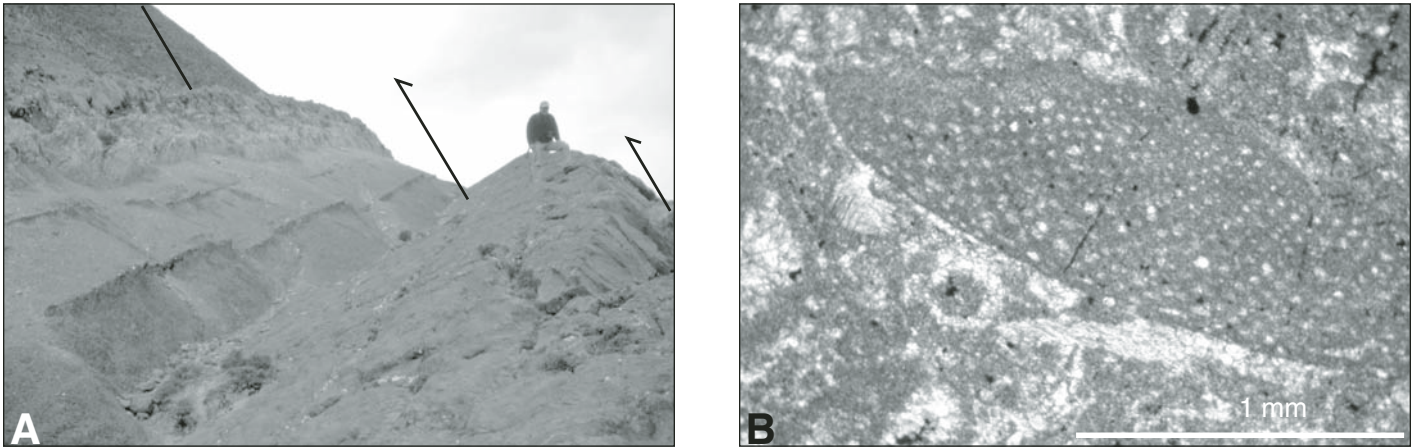


Figure 7. Photos of the Penbo Member of the Takena Formation. (A) Carbonate parasequence (beds are dipping to the left, person for scale). The Penbo Member contains a series of stacked parasequences that consist of, from base to top, marly siltstone and carbonate mudstone, orbitolinid-wackestone, and an orbitolinid and bivalve packstone. (B) Orbitolinid fossil in a petrographic thin section of the limestone within the Penbo Member of the Takena Formation (plane light).

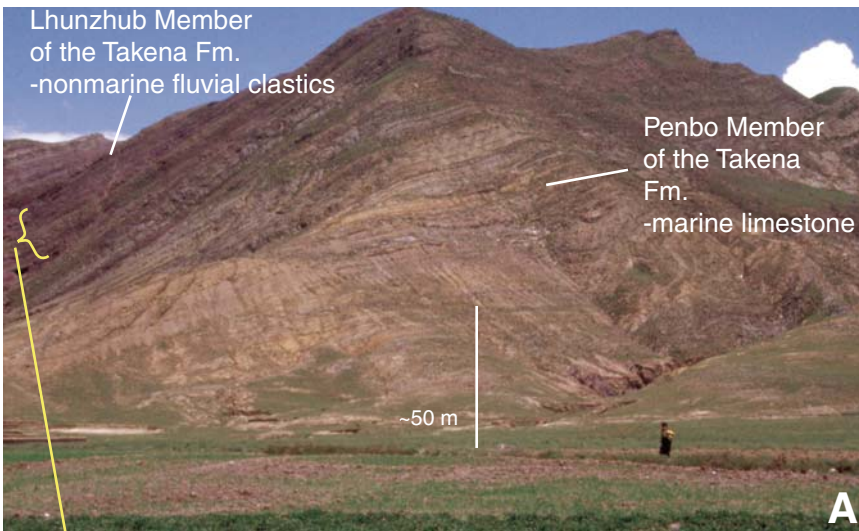
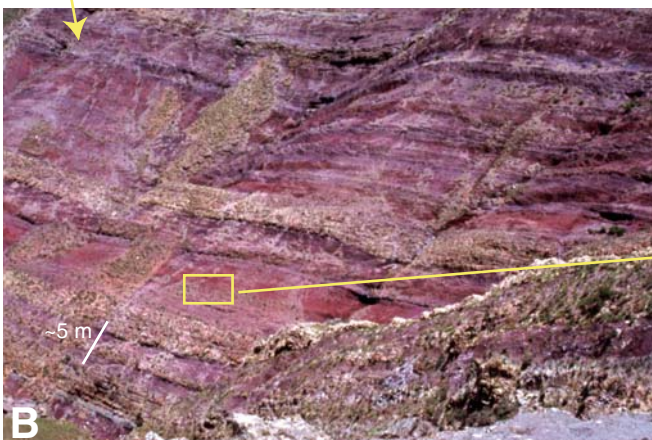


Figure 8. Lower part of the Takena Formation: Penbo Member of the Takena Formation and the overlying terrestrial red beds of the Lhunzhub Member in the Penbo area (see also Fig. 5). (A) An overview of the transition from the shallow-marine limestone beds to the Lhunzhub Member (beds are dipping to the left). (B) Photo of the terrestrial red beds overlying the Penbo Member (beds are dipping into the page and to the right). Note the numerous stacked horizons of red-purple siltstone, which are interpreted as paleosols horizons. (C) Close-up of paleosol deposits (beds are dipping into the page and to the right). Note the massive nature of the siltstone and the CaCO_3 nodules.



carbonate mudstone (lithofacies C2). Unlike the limestone beds at the base of the Takena Formation, these deposits do not contain organized parasequences and lack orbitolinid tests or microfossils other than oysters.

**Middle Limestone Lithofacies Association—
Interpretation**

The middle limestone lithofacies association is interpreted as having been deposited in a low-energy, marginal-marine environment, most likely one with estuarine or lagoonal character-

istics. Low-diversity fossil assemblages that are dominated by oysters and fine-grained sediment are common in estuarine/lagoonal environments (e.g., Tucker and Wright, 1990).

**Middle Siltstone Lithofacies Association—
Description**

Conformably overlying the middle limestone lithofacies association is the middle siltstone lithofacies association, which consists of a thick succession of monotonous red siltstone with minor amounts of sandstone and local limestone beds

(Figs. 6 and 9). The red siltstone typically lacks bedding and does not contain CaCO₃ nodules (lithofacies F2). The majority of the siltstone has a pervasive cleavage, making the identification of sedimentary structures difficult. Sandstone beds are fine-grained and contain unidirectional current ripples, climbing ripples, occasional convoluted bedding, and small trough cross-stratification (set thickness <0.5 m). Also within this lithofacies association are 2–6-m-thick, upward-fining sandstone units that overlie minor scour surfaces and contain trough cross-stratification and abundant unidirectional current ripples and climbing ripples. Sandstone within the lithofacies association contains little to no evidence of bioturbation. The qualitative sandstone/mudstone ratio within this lithofacies association is relatively low (e.g., Figs. 6 and 9). Locally, the middle siltstone lithofacies association contains thin and laterally continuous beds of ostracode-bearing limestone and laminated marly-siltstone.

**Middle Siltstone Lithofacies Association—
Interpretation**

The features within this succession and its stratigraphic proximity to underlying oyster-bearing limestone beds suggest a lower coastal plain depositional environment. The principal depositional components are interpreted to have been nonmigrating streams and interfluvial floodplain areas with small lakes. The thin- and thick-bedded sandstone with unidirectional current ripples and climbing ripples is interpreted as crevasse splay and channel levee deposits. The 2–6-m-thick sandstone units encased within the siltstone are interpreted as deposits of relatively fixed channel rivers, most similar to anastomosing streams (e.g., Smith and Smith, 1980). Similar fluvial channels with well-developed levees are common in modern and ancient lower coastal plain environments (e.g., Törnqvist, 1993). The siltstone was deposited in floodplains within low-lying coastal plain areas that were inundated by crevasse splay events (e.g., Elliot, 1974). The ostracode limestone and laminated siltstone are interpreted as deposits of lower coastal plain lacustrine environments.

**Upper Fluvial Lithofacies Association—
Description**

The uppermost interval of the Takena Formation consists of thick sandstone units and interstratified red mudstone beds of the upper fluvial lithofacies association (Figs. 6 and 9); in many locations, the Takena Formation is unconformably overlain by volcanic strata of the Linzizong Formation (Fig. 10). The sandstone units of the upper fluvial lithofacies association are in many ways identical to the type-B sandstone units within the lower fluvial lithofacies association

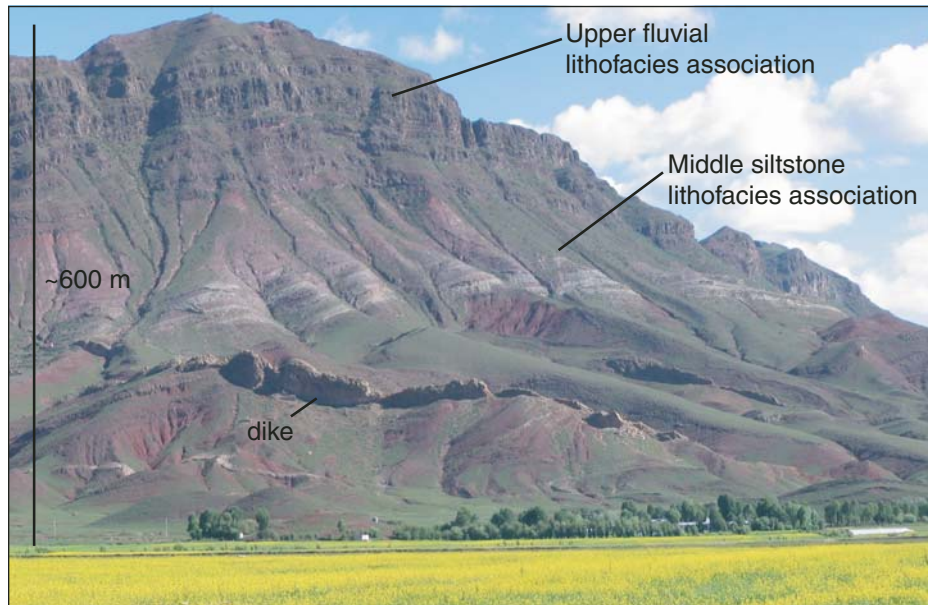


Figure 9. Upper part of the Takena Formation: overview of the upper part of the Lhunzhub member of the Takena Formation (beds are dipping to the left; see also Fig. 6). Thick fluvial sandstone sequences overlie a succession of siltstone and fine-grained sandstone.

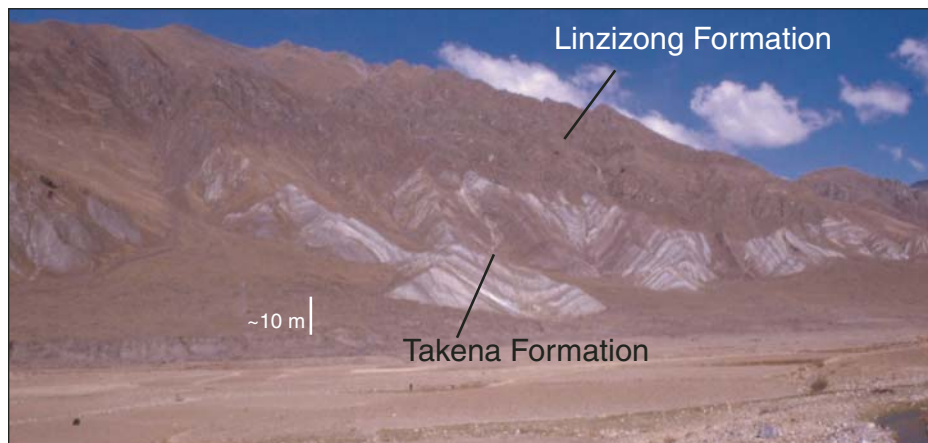


Figure 10. Takena and Linzizong Formations. Folded beds of the Takena Formation are overlain by relatively undeformed volcaniclastic beds of the Linzizong Formation in the Maqu area; vertical relief of exposure is roughly 300 m. Ages of the Linzizong Formation indicate that deformation of the Takena Formation occurred prior to 69 Ma.

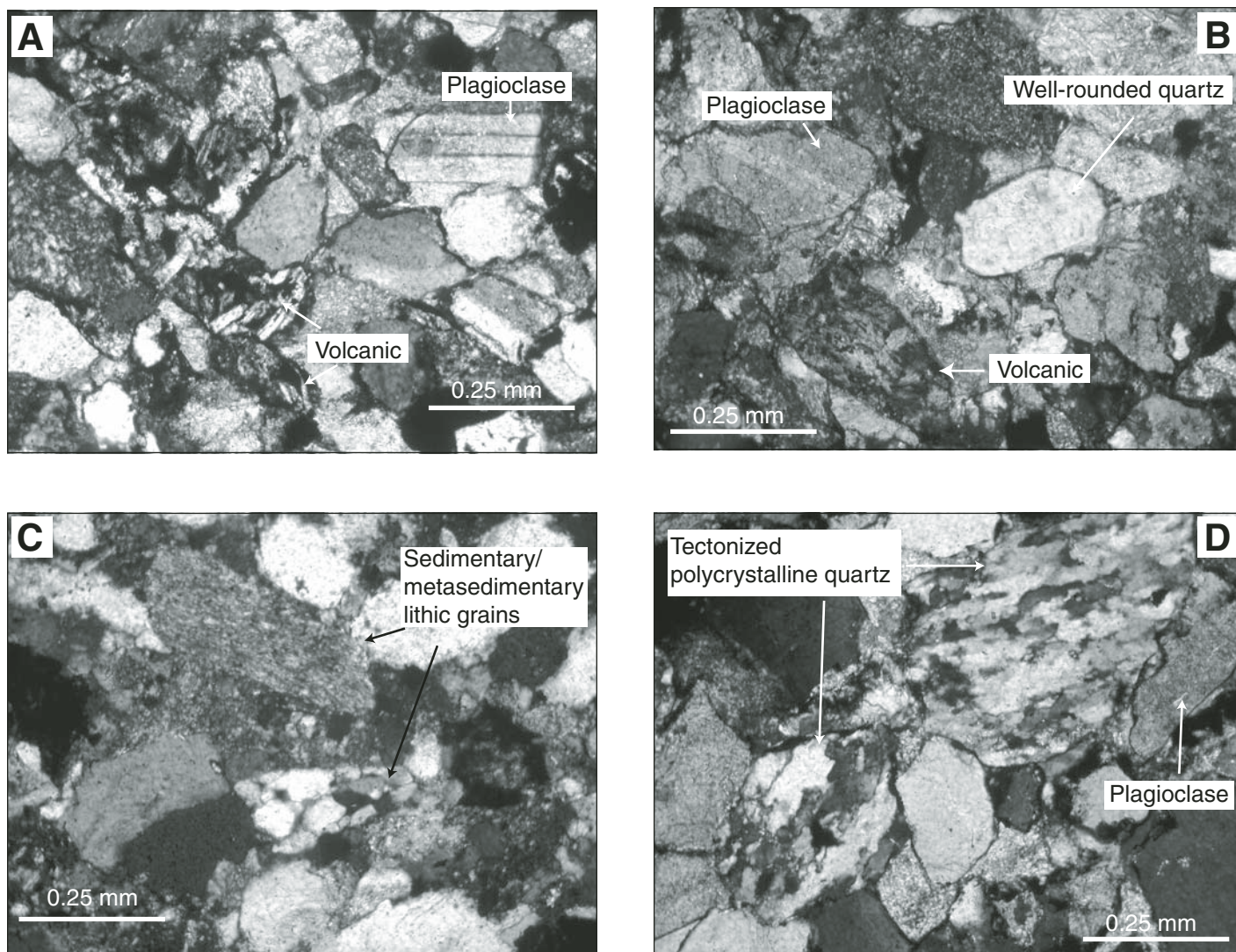


Figure 11. Petrography: Photos of petrographic thin sections of sandstone from the Takena Formation (all photos in cross-polarized light). (A) Example of a typical sandstone within the Takena Formation. (B) Well- to very well-rounded quartz grains surrounded by unstable lithic volcanic grains and plagioclase, suggesting that the quartz has been recycled. (C) Sedimentary/metasedimentary lithic grains are common within the Takena Formation. (D) Two tectonized polycrystalline quartz grains from the Takena Formation.

discussed already, and therefore will be described only briefly. The sandstone units consist of multiple, stacked, 2–4-m-thick, medium-grained, trough cross-stratified sandstone packages (lithofacies S1). Unlike the lower fluvial lithofacies association, where the type-B sandstone units are rare and <10 m thick, the type-B sandstone units are ubiquitous within the upper fluvial lithofacies association and also tend to be coarser-grained and much thicker than 10 m (cf. Figs. 5 and 6). The successions within the Maqu region are composed of similar sandstone units, but they also contain occasional clast-supported pebble-conglomerate beds.

Mudstone beds within the upper fluvial succession are massive and in many ways similar to

mudstone in the lower fluvial lithofacies association (see previous); however, the mudstone intervals in the upper fluvial lithofacies association typically lack CaCO_3 nodules. The relative proportion of sandstone to mudstone is noticeably higher within the upper fluvial lithofacies association compared to the lower fluvial lithofacies association (cf. Figs. 5 and 6).

Upper Fluvial Lithofacies Association— Interpretation

Similar in almost all respects to the type-B sandstone units of the lower fluvial lithofacies association, the sandstone units of the upper fluvial succession are interpreted as deposits of sandy braided streams (for a detailed

interpretation with associated references, see the lower fluvial lithofacies association in the previous paragraphs). The mudstone is interpreted as having been deposited in floodplain environments adjacent to the fluvial channels.

PALEOCURRENT DATA

Paleocurrent data consist of measurements made from 572 limbs of trough cross-stratification sets and 21 primary current lineations preserved within upper Cretaceous fluvial sandstone units. The orientations of cross-stratification sets were measured following method I of DeCelles et al. (1983). Overall, the paleocurrent data record north-northwest-directed sediment

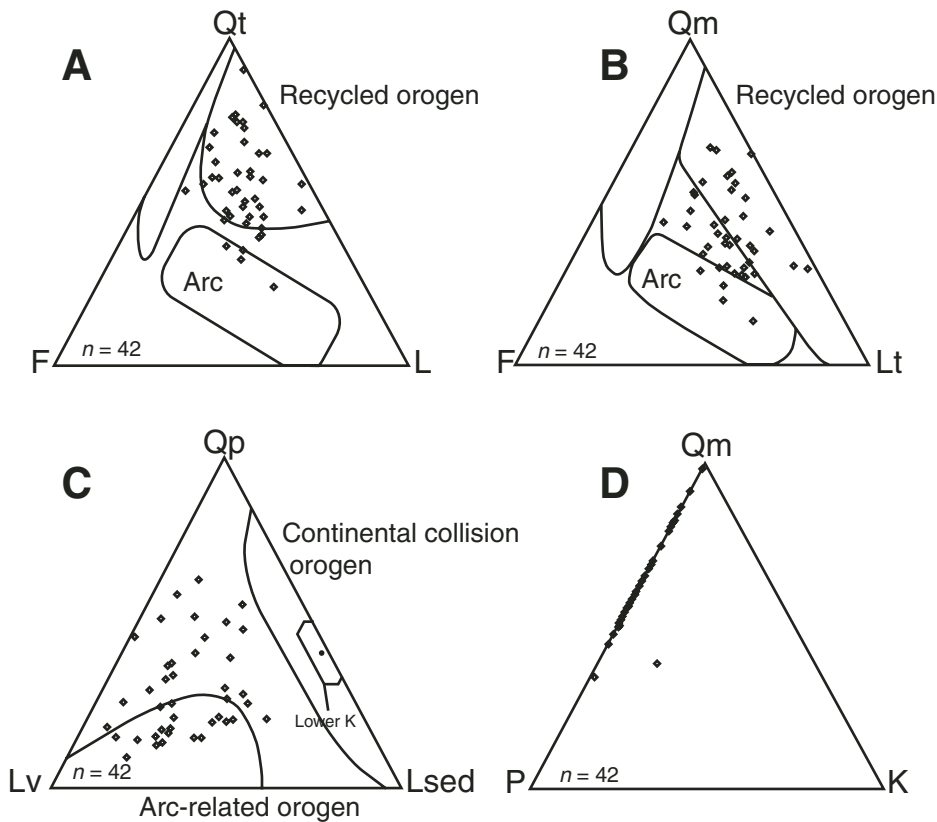


Figure 12. Sandstone composition: QFL diagrams constructed from point-counting 42 thin sections of Tadena Formation sandstone. Qt—total quartz, F—feldspar, L—lithics, Qm—monocrystalline quartz, Lt—total lithics, Qp—polycrystalline quartz, Lv—volcanic lithics, Lsed—sedimentary lithics; see GSA Data Repository for a complete explanation of modes (see text footnote 1). (A–B) Sandstone composition of the Tadena Formation generally plots within or near the recycled orogen field (fields from Dickinson and Suczek, 1979). (C) Sandstone of the Tadena Formation contains abundant lithic-volcanic grains, suggesting an arc-related source. The average composition of the underlying lower Cretaceous sandstone (and 1 standard deviation) is also shown to highlight the contrast in composition between the two stratigraphic successions. (D) Relative amounts of monocrystalline quartz (Qm), plagioclase (P), and potassium feldspar (K) within the Tadena Formation.

transport during the Late Cretaceous (Figs. 5 and 6). In the Penbo area, paleocurrent directions near the base of the Tadena Formation range from southwest- to northeast-directed, but primarily indicate north-northwest-directed transport. Sandstone units near the base of the Tadena Formation in the Maqu area contain more north- and northeast-directed indicators than the lowermost sandstone units of the Penbo area, and in general record sediment transport to the north. Paleocurrent directions in the upper portion of the Tadena Formation indicate that transport was almost exclusively to the northwest and varied little (Fig. 6). Based on the paleocurrent data, sediment transport in the Nam Co area was also northwest-directed. Overall, the paleocurrent data indicate that sediment of the Tadena

Formation was derived from an area approximately south-southeast of the Penbo, Maqu, and Nam Co locales. The Late Cretaceous paleogeography suggested by these data is significantly different from existing models, which depict sediment as having been transported from north to south, through the Gangdese arc, and deposited in the Xigaze forearc basin (e.g., Leeder et al., 1988; Dürr, 1996).

PETROGRAPHY

Description

Standard petrographic thin sections were made from 42 medium-grained sandstone samples that were collected while measuring

stratigraphic sections. The thin sections were stained for potassium and calcium feldspar and point-counted (450 counts per slide) using a modified Gazzi-Dickinson method (Ingersoll et al., 1984); the modification involves the identification of monocrystalline quartz grains that are part of sedimentary lithic fragments. The petrographic counting parameters are included in the GSA Data Repository, as are the raw point-count data (Table DR1¹).

Sandstone within the Tadena Formation consists of calcite-cemented feldspathic litharenite and litharenite beds, which have average modal compositions of Qm:F:Lt = 41:18:41, and Qt:F:L = 55:19:26 (Figs. 11 and 12). Sub-angular to well-rounded monocrystalline quartz is the primary constituent of total quartz within the samples. Sandstone units in the Penbo area have the highest percentage of total quartz, and those in the Maqu area have the lowest. Feldspar content is uniform between the different locations and sections (~19% of modal composition), and, with the exception of one unit in the Maqu area, consists entirely of plagioclase feldspar (Fig. 11). Volcanic fragments are the predominant lithic grain within the Tadena Formation, and constitute an average of 17% of total framework grains (Fig. 12). Volcanic grains are typically andesitic and often contain microlaths of plagioclase feldspar (Fig. 11). In addition to volcanic grains, the sandstone contains lithic grains derived from sedimentary and metamorphosed strata, including phyllite, mudstone, sandstone, and quartzite (Fig. 11). Lithic fragments of calcium carbonate are typically micritic, and occasionally contain unidentifiable bioclasts. Tourmaline, epidote, and zircon are the most common accessory minerals.

Interpretation

The composition of sandstone within the Tadena Formation is most similar to sandstone derived from arc-related recycled orogens (Fig. 12). Potential source rocks in the southern Lhasa terrane include: metamorphosed and unmetamorphosed Carboniferous mudstone and quartzose sandstone; local Permian limestone; Triassic limestone, volcanoclastic strata, and basalt; Jurassic limestone and mudstone; Early Cretaceous quartzose sandstone, mudstone and limestone; and granites, granodiorites and volcanic strata of Early to Late Cretaceous age (Kidd et al., 1988; Yin et al., 1988; Liu, 1988; Leeder et al., 1988).

¹GSA Data Repository item 2007004, sandstone petrography, is available on the Web at <http://www.geosociety.org/pubs/ft2007.htm>. Requests may also be sent to editing@geosociety.org.

Abundant volcanic and plagioclase grains within the Takena Formation suggest that the Late Cretaceous Gangdese volcanic arc was an important sediment source for the upper Cretaceous strata. In addition to these grains, it is likely some of the quartz grains in the Takena Formation were also derived from the Gangdese arc. Lithic grains of sandstone, limestone, mudstone, and phyllite are interpreted as being derived from Paleozoic and Mesozoic sedimentary cover strata exposed along the southern portion of the Lhasa terrane (Fig. 11). The presence of well-rounded quartz grains in compositionally immature sandstone suggests at least some of the quartz in the Takena Formation was recycled from underlying quartzose sedimentary units, like those within the Carboniferous strata (Fig. 11). This idea is supported by the fact that in some areas, Cretaceous rocks unconformably overlie Carboniferous strata (Kidd et al., 1988), and the distribution of U-Pb ages of detrital zircons from the Takena Formation is similar to that of Carboniferous sandstone (Leier et al., 2004; Leier, 2005), which suggests that Carboniferous strata was exposed and was being eroded before and/or during Cretaceous time. With respect to the abundance of plagioclase, not all of these grains within the Takena Formation were necessarily derived from arc-volcanic rocks. Plagioclase-rich Triassic volcanoclastic strata are exposed in the southern Lhasa terrane (Fig. 1) and could have been a source of sediment for upper Cretaceous strata.

Several aspects of the Takena Formation sandstone exposed in the Maqu area suggest that the sediment deposited in this region had a slightly different provenance than similar strata exposed in the Penbo and Nam Co locations (Table DR1 [see footnote 1]). Relative to sandstone compositions at all of the other locations, sandstone in the Maqu area has the highest percentage of volcanic fragments, the largest amount of tectonized polycrystalline grains and recycled sandstone fragments, and Maqu is the only location where sandstone beds contain grains of potassium feldspar. Grain-size, paleocurrent directions, and fluvial facies within the Takena Formation in the Maqu region also differ slightly from those features in the Takena Formation in the Penbo and Nam Co locales. The relatively high percentage of tectonized quartz and the presence of potassium feldspar grains imply that the fluvial systems that traversed the Maqu area may have been draining a more dissected region of the source area (e.g., Dickinson and Suczek, 1979).

SUBSIDENCE

The Late Jurassic–Eocene subsidence history of the southern Lhasa terrane has been

reconstructed using stratigraphic data from this study and from the literature (Leeder et al., 1988; Yin et al., 1988). Late Jurassic–Eocene strata were decompacted following the methods outlined in Allen and Allen (1990), and tectonic subsidence was calculated using the techniques described in Allen and Allen (1990) and Angevine et al. (1990).

The subsidence history associated with the Cretaceous–Eocene deposits of the southern Lhasa terrane is displayed in Figure 13. Relatively poor age control exists for the fluvial deposits of the Takena Formation (Lhunzhub Member), so the decompacted stratigraphic thickness curve was calculated using various depositional durations. The general character of the subsidence curve remains the same regardless of the depositional duration—the shorter the period of deposition, the steeper the curve. Subsidence rates were constant during latest Jurassic and earliest Cretaceous time, but decreased during Aptian and Albian time (Fig. 13). Beginning in the Late Cretaceous, subsidence rates increased and continued at high levels through Paleocene time. The subsidence curve calculated for southern Lhasa exhibits an overall convex-upward shape typical of subsidence histories in foreland basins (e.g., Angevine et al., 1990). In foreland basin settings, this subsidence history is ascribed to initial deposition within a slowly subsiding backbulge or forebulge depozone followed by

deposition within a foredeep depozone under increasing subsidence rates (e.g., DeCelles and Giles, 1996).

Several aspects of the subsidence history warrant further consideration. No constraints on surface paleoelevation exist for the time period encompassing deposition of the terrestrial red beds of the Takena Formation. Estuarine/lagoonal limestone beds within the middle portion of the Takena Formation imply that the succession was deposited near sea level, at least during deposition of the lower half of the formation. Any increase in surface elevation that occurred during deposition of the Takena Formation, or the Linzizong Formation, would reduce the slope of the subsidence curve during the latter stages of deposition. Eustatic sea-level changes were also not taken into account, which again, could reduce the amount of calculated tectonic subsidence. However, we suspect that the total subsidence and subsidence rates calculated for the Cretaceous–Eocene strata are conservative estimates. A thicker stratigraphic succession or a briefer depositional period would have the effect of increasing the total amount of subsidence and the subsidence rates. The upper surface of the Takena Formation is a regional unconformity; hence, the total thickness of the Takena Formation is unknown, and the ~2 km of strata exposed today represent a minimum thickness. Similarly, the 3 km of volcanoclastic

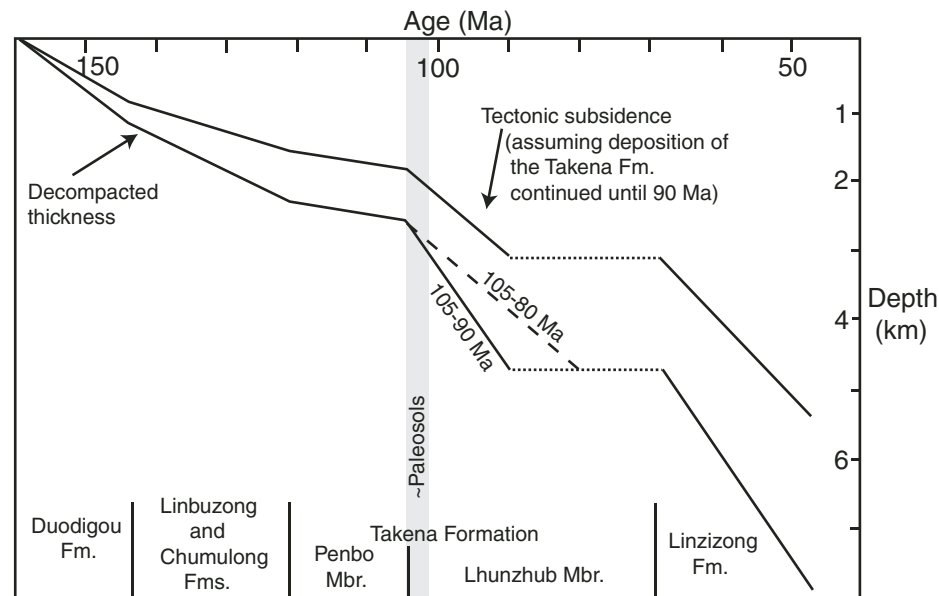


Figure 13. Subsidence: Decompacted thickness and tectonic subsidence curve for Cretaceous strata in the southern portion of the study area (Penbo and Maqu areas). Because of poor age control, the decompacted thickness of the Takena Formation is displayed with alternative durations of deposition. The horizontal dashed lines represent periods for which there is no sedimentary record. Overall, the curve is most similar to those from foreland basin settings. See text for further discussion.

sediment of the Linzizong Formation may have once been as thick as 6 km or more (e.g., Copeland et al., 1995), although whether these strata were deposited in a foredeep/wedgetop depozone is uncertain. Future studies using various indices of thermal maturity could help to shed light on the former thickness of the strata in the region. Folded beds of the Takena Formation that underlie flat-lying beds of the Linzizong Formation (69 ± 2.4 Ma; He, 2005) obviously require that deposition of the Takena Formation must have ceased before ca. 69 Ma. A 90 Ma dike crosscuts an unspecified section of the Takena Formation (Coulon et al., 1986), suggesting that the cessation of deposition was closer to 90 Ma than 69 Ma. Therefore, the decompacted thickness curve calculated using a 15 m.y. duration (ca. 105–90 Ma) is probably more realistic than the curve calculated for a longer duration (e.g., 105–80 Ma; Fig. 13).

PALEOGEOGRAPHY AND TECTONIC SETTING

Reconstructions of the paleogeography and tectonic setting of the central-southern portion of the Lhasa terrane are shown in Figure 14. The temporal evolution is constrained by the relative stratigraphic position of particular lithofacies associations, and absolute ages are delimited by fossil data from limestone within the Takena Formation and zircon crystallization ages from samples of the overlying Linzizong Formation (e.g., He, 2005). The major paleogeographic features within the reconstructions (e.g., fluvial systems) are directly supported by evidence presented within this paper, or are otherwise noted as being inferred from other data (e.g., paleoshoreline trends).

A Retroarc Foreland Basin

The sedimentary characteristics of the Takena Formation indicate that deposition occurred in a retroarc foreland basin. The modal composition of sandstone within the Takena Formation is most similar to retroarc foreland basin deposits (Fig. 12; e.g., Dickinson and Suczek, 1979; DeCelles and Hertel, 1989; Jordan, 1995). The overall upward-coarsening nature of the formation and the upward increase in sandstone thickness and sandstone/mudstone ratio are also common features of foreland basin strata (e.g., Willis, 1993a, 1993b). The temporal and spatial pattern (south-to-north) of clastic deposition is consistent with a foreland basin model (Figs. 3 and 14), as are the convex-upward subsidence curve (Fig. 13), and paleocurrent data (Figs. 5 and 6). With respect to the paleo-stress field, undeformed strata of the Linzizong

Formation (69–48 Ma; He, 2005) that overlie folded beds of the Takena Formation unequivocally record Late Cretaceous crustal shortening in the Gangdese retroarc region (Fig. 10). Folded and faulted foreland basin strata are common in almost all retroarc foreland basin systems. Together, the sedimentological and structural characteristics of the Takena Formation are consistent with a northward-migrating fold-and-thrust belt and foredeep.

Lower Strata of the Takena Formation

The lower strata of the Takena Formation refer to the limestone beds of the Penbo Member, and the overlying marginal-marine siltstone and lower fluvial lithofacies associations. Deposition of the Takena Formation initiated in Aptian time as southern Tibet was submerged beneath a shallow epeiric sea dominated by muddy lagoonal environments and sporadic rudist patch reefs (Fig. 14). Northward-flowing streams delivered clastic material to the area, although the influx of this sediment was relatively insignificant compared to the volume and rate of carbonate deposition. The depiction of an east-west-trending paleoshoreline located south of the study area is based on the relative abundance of interbedded clastic deposits in more southerly exposures (Penbo and Maqu areas) and an inferred paleoshoreline trend that was roughly perpendicular to the fluvial paleocurrent direction (northward-directed; see Fig. 5). Aptian-Albian clastic strata with volcanic detritus and north-directed paleocurrent indicators, and the coeval formation of the Xigaze forearc basin (Dürr, 1996) indicate that a nascent Gangdese magmatic arc had developed south of the study area by this time.

By the end of the Albian, clastic material from the south began to infill the region from south to north (Fig. 14). Clastic, shallow-marine environments replaced carbonate environments in the south, although in northern portions of the Lhasa terrane, carbonate deposition continued into the Cenomanian (Yin et al., 1988). Eventually, the influx of clastic sediment overwhelmed the marine accommodation, and terrestrial depositional environments occupied the entire area, with the possible exception of the northernmost parts of the Lhasa terrane. North-northwest-flowing meandering rivers traversed the Penbo area, whereas contemporaneous rivers in the Maqu area were more similar to braided streams and most likely originated from a different watershed than the Penbo fluvial system. Multiple episodes of soil formation occurred in the floodplain areas adjacent to the fluvial channels.

The lowermost limestone beds of the Penbo Member and the overlying marginal-marine

siltstone and paleosol-rich fluvial strata are interpreted as backbulge-forebulge deposits of a foreland basin (Fig. 14). The lithofacies of the carbonate strata and the relatively low rate of subsidence in the area during their deposition correlate well with backbulge-forebulge deposits from modern and ancient foreland basins (e.g., Dorobek, 1995; DeCelles and Giles, 1996). The numerous paleosols within the terrestrial strata overlying the limestone beds also suggest a forebulge depozone, where low sediment accumulation rates often result from long-wavelength, low-amplitude flexural uplift and the consequent loss of accommodation (Fig. 14; e.g., DeCelles and Giles, 1996).

Middle Strata of the Takena Formation

The middle strata of the Takena Formation, which overlie the marine limestone and paleosol-rich fluvial strata, consist of the middle siltstone and middle marine limestone lithofacies association. This interval is dominated by fine-grained strata that were deposited in a lower coastal plain environment (Fig. 14). The paleogeography during deposition of these strata was characterized by anastomosing fluvial channels, with local estuarine conditions, and local lakes in the interfluvial region (Fig. 14).

The middle strata of the Takena Formation are interpreted as distal foredeep deposits (Fig. 14). Relative to the underlying paleosol deposits, the sedimentary characteristics of the middle strata suggest that an increase in the accommodation/sedimentation ratio occurred during deposition of these strata (e.g., Törnqvist, 1993); the decompacted thickness of the strata indicates that the subsidence rate increased during this period as well (Fig. 13). Fine-grained lower coastal plain and anastomosing fluvial deposits are common in distal foredeep locations (e.g., Shuster and Steidtmann, 1987), where subsidence rates increase (relative to the forebulge depozone) and the influx of sediment remains low (relative to proximal parts of the foredeep).

Upper Strata of the Takena Formation

The upper strata of the Takena Formation refer to the upper fluvial lithofacies association. The paleogeography during deposition of these strata was dominated by northwest-flowing sandy braided river systems (Fig. 14). Whether this area was occupied by a single river system or multiple systems with similar characteristics and flow directions is not discernible at present. The different sandstone composition in the Maqu area relative to the other studied sections suggests that the rivers in this location were draining a different source area.

The upward-coarsening upper strata of the Takena Formation are interpreted as proximal foredeep deposits. The depositional environments, provenance, and large-scale fluvial architecture of the Takena Formation, which progresses from fine-grained, anastomosing, and meandering stream deposits in the lower and middle portion of the succession to multi-story and multilateral braided stream sandstone units near the top, are very similar to many well-documented nonmarine foreland basin successions (e.g., Willis 1993a, 1993b; Horton and DeCelles, 2001).

Deformation of the Takena Formation

Following deposition of the upper fluvial succession but before ca. 70 Ma, the beds of the Takena Formation were folded, partially eroded, and then buried by volcanic flows and tuffs of the Linzizong Formation (Figs. 10 and 14). This nondepositional history of the Takena Formation is interpreted as recording the incorporation of these strata into a basinward migrating fold-and-thrust belt (Fig. 14).

DISCUSSION

The Migration of a Deformation Front

A simple test of the foreland basin interpretation can be performed by estimating the rate at which a foreland basin and the associated deformation front (i.e., fold-and-thrust belt) must have moved in order to account for the sedimentology and deformational history of the Takena Formation (Fig. 14). These rates can be compared with values calculated from known retroarc foreland basins. We use the following parameters to make a first-order estimation of the migration rate: the distance between the deformation front and the forebulge crest is 200–300 km; deposition on the forebulge crest occurred at roughly 105 Ma (end of the Albian and roughly coeval to deposition of the lower fluvial lithofacies association; Fig. 14); and the deformation front reached the Penbo and Maqu locations by 70 Ma (oldest age of the Linzizong Formation overlying folded Takena Formation beds; Fig. 14). Using these values, the migration rate of the flexural wave (i.e., rate of the advancing fold-and-thrust belt) was 6–9 mm/yr. Using a more restricted time interval between forebulge deposition and deformation of the Takena Formation of 15 m.y. (105–90 Ma) yields rates of 14–20 mm/yr. It should be emphasized that we are not implying that these values are the actual migration rates. The significance of these values is that they are similar to rates of frontal thrust belt migration as derived

from modern global positioning system (GPS) measurements and from ancient foreland basin strata (e.g., Norabuena et al., 1998; DeCelles and Horton, 2003), which means our foreland basin interpretation is plausible.

Where is the Cretaceous Fold-and-Thrust Belt?

By definition, the presence of a Late Cretaceous retroarc foreland basin in southern Tibet requires that a retroarc fold-and-thrust belt was actively deforming in southern Tibet during the same time. Although such a feature has been hypothesized to have existed (e.g., Burg, et al., 1983; Allegre et al., 1984; England and Searle, 1986), no such fold-and-thrust belt has yet been unequivocally identified. However, previous and more recent studies of the Lhasa terrane have yielded more definitive evidence that a Cretaceous-aged “Gangdese retroarc fold-and-thrust belt” did exist along the southern margin of the Lhasa terrane (England and Searle, 1986; Kapp et al., 2004). Interformational relationships provide ample evidence that the Takena Formation was folded during the Late Cretaceous, and deformation records at least 26%–50% Late Cretaceous shortening (Fig. 10; Burg et al., 1983; Pan, 1993; Kapp et al., 2004). The intensity of this deformation decreases from south to north (Burg et al., 1983; Coward et al., 1988), which is consistent with a north-verging retroarc fold-and-thrust belt. Structural relationships, in conjunction with recently discovered kinematic indicators, suggest that north-verging thrust sheets were active in the southern portion of the Lhasa terrane during the Late Cretaceous (Kapp et al., 2004; He, 2005). Furthermore, magmatic evidence indicates that by at least 80 Ma, crust in parts of the southern Lhasa terrane was abnormally thick (Wen et al., 2004). Considering these observations and the results of this study, we postulate that future studies will find more conclusive evidence of a Cretaceous fold-and-thrust belt in southern Tibet.

Implications for Plateau Development

The marked difference between the extent of deformation in the Cretaceous Takena Formation and the overlying Late Cretaceous–Paleocene Linzizong Formation (Fig. 10; e.g., Pan, 1993) has led to the hypothesis that prior to the collision with India, the crust of southern Asia had obtained topographic elevations and buoyancy forces of sufficient magnitude such that horizontal forces produced during the Indo-Asian collision were transmitted inboard (to the north) and not absorbed via internal strain (England and Searle, 1986). The evidence of a

retroarc foreland basin in southern Tibet is consistent with Late Cretaceous thickening of the region prior to the Indo-Asian collision. Cretaceous marine limestone is commonly invoked as evidence that southern Asia was at or near sea level prior to the Indo-Asian collision. However, within southern Tibet, the youngest limestone is Cenomanian in age (Smith and Xu, 1988), which leaves a significant period of time (~40 m.y.) before the Indo-Asian collision when considerable surface and rock uplift may have occurred. Moreover, the presence of marine lithofacies does not necessarily support low regional elevations, as is evidenced in many modern contraction-related orogens where high topography is flanked by areas below sea level.

CONCLUSIONS

The Takena Formation of the Lhasa terrane in southern Tibet is composed of a lowermost marine limestone member and an overlying clastic member that together are ~2 km thick. The limestone beds were deposited within a shallow-marine, lagoonal environment that was eventually inundated by clastic sediment derived from southern source areas. The overlying clastic strata consist of fluvial sandstone units and floodplain mudstone. Paleocurrent data indicate that the fluvial systems transported sediment from the south-southeast to the north-northwest. Petrographic data indicate that the strata of the Takena Formation were derived primarily from a Late Cretaceous volcanic arc (Gangdese arc) that was located along the southern margin of the Lhasa terrane, although pre-Late Cretaceous sedimentary cover strata also served as a sediment source. The shallow-marine seaway that occupied the region during the Aptian–Albian was eventually infilled by clastic material from south to north. Subsidence rates were initially low during deposition of the limestone but increased noticeably during deposition of the overlying terrestrial clastic deposits. Taken together, all of the data indicate that the Takena Formation was deposited in retroarc foreland basin. This requires the existence of a Cretaceous retroarc fold-and-thrust belt within the southern portion of the Lhasa terrane and also implies that southern Tibet had a thickened crust before the Indo-Asian collision.

ACKNOWLEDGMENTS

This research was supported by the U.S. National Science Foundation grant (EAR-0309844), Geological Society of America, and American Association of Petroleum Geologists student grants, and an National Security Education Program [NSEP] Boren Fellowship from the U.S. Department of Defense. Support was also provided by grants from ExxonMobil and Chevron. This work benefited from discussions with

many students and faculty members in the Department of Geosciences at the University of Arizona. We thank Shundong He, Dan Eisenberg, John Volkmer, Alex Pullen, Jessica Kapp, Jerome Guynn, Matt Fabijanac, Zhou Ma, and Wang Zhu for assistance in the field, Dave Barbeau and Facundo Fuentes for helpful discussions, and Dick Hay for help with the petrographic work. We thank R.W. Scott for his help in examining some of the paleontological samples. This manuscript benefited from comments on an earlier draft by George Gehrels, George Zandt, and Jay Quade. We thank Brian Darby, Peter Cawood, and an anonymous reviewer for their thoughtful and helpful reviews.

REFERENCES CITED

Achache, J., and Courtillot, V., 1984, Paleogeographic and tectonic evolution of southern Tibet since middle Cretaceous time: New paleomagnetic data and synthesis: *Journal of Geophysical Research*, v. 89, p. 10,311–10,339.

Allégre, C.J., and 34 others, 1984, Structure and evolution of the Himalaya-Tibet orogenic belt: *Nature*, v. 307, p. 17–22.

Allen, J.R.L., 1964, Studies in fluvial sedimentation: Six cyclothems from the lower Old Red Sandstone, Anglo-Welsh basin: *Sedimentology*, v. 3, p. 163–198, doi: 10.1111/j.1365-3091.1964.tb00459.x.

Allen, J.R.L., 2001, Principles of Physical Sedimentology: Caldwell, New Jersey, The Blackburn Press, 272 p.

Allen, P.A., and Allen, J.R., 1990, Basin Analysis, Principles and Applications: Cambridge, Massachusetts, Blackwell Science, 451 p.

Angevine, C.L., Heller, P.L., and Paola, C., 1990, Quantitative sedimentary basin modeling: American Association of Petroleum Geologists, Course Notes 32, 132 p.

Beck, S.L., and Zandt, G., 2002, The nature of orogenic crust in the central Andes: *Journal of Geophysical Research*, v. 107, no. B10, 2230, doi: 10.1029/2000JB000124.

Besse, J., and Courtillot, V., 1988, Paleogeographic maps of the continents bordering the Indian Ocean since the Early Jurassic: *Journal of Geophysical Research*, v. 93, p. 11,791–11,808.

Bristow, C.S., 1993, Sedimentary structures exposed in bar tops in the Brahmaputra River, Bangladesh, in Best, J.L., and Bristow, C.S., eds., Braided Rivers: The Geological Society of London Special Publication 75, p. 277–290.

Burg, J.P., and Chen, G.M., 1984, Tectonics and structural zonation of southern Tibet, China: *Nature*, v. 311, p. 219–223, doi: 10.1038/311219a0.

Burg, J.-P., Proust, F., Tapponnier, P., and Ming, C.G., 1983, Deformation phases and tectonic evolution of the Lhasa block (southern Tibet, China): *Eclogae Geologicae Helveticae*, v. 76, p. 643–665.

Butler, R., 1995, When did India hit Asia?: *Nature*, v. 373, p. 20–21, doi: 10.1038/373020a0.

Cant, D.J., and Walker, R.G., 1978, Fluvial processes and facies sequences in the sandy braided South Saskatchewan River, Canada: *Sedimentology*, v. 25, p. 625–648, doi: 10.1111/j.1365-3091.1978.tb00323.x.

Chen, Y., Courtillot, V., Cogne, J.-P., Besse, J., Yang, Z., and Enkin, R., 1993, The configuration of Asia prior to the collision of India: Cretaceous paleomagnetic constraints: *Journal of Geophysical Research*, v. 98, p. 21,927–21,941.

Copeland, P., Harrison, T.M., Pan, Y., Kidd, W.S.F., Roden, M., and Zhang, Y., 1995, Thermal evolution of the Gangdese batholith, southern Tibet: A history of episodic unroofing: *Tectonics*, v. 14, p. 223–226, doi: 10.1029/94TC01676.

Coulon, C., Maluski, H., Bollinger, C., and Wang, S., 1986, Mesozoic and Cenozoic volcanic rocks from central and southern Tibet: ^{39}Ar - ^{40}Ar dating, petrological characteristics and geodynamical significance: *Earth and Planetary Science Letters*, v. 79, p. 281–302, doi: 10.1016/0012-821X(86)90186-X.

Coward, M.P., Kidd, W.S.F., Yun, P., Shackleton, R.M., and Hu, Z., 1988, The structure of the 1985 Tibet Geotraverse, Lhasa to Golmud: *Philosophical Transactions of the Royal Society of London, ser. A, Mathematical and Physical Sciences*, v. 327, p. 307–336.

DeCelles, P.G., Langford, R.P., and Schwartz, R.K., 1983, Two new methods of paleocurrent determination from trough cross-stratification: *Journal of Sedimentary Petrology*, v. 53, p. 629–642.

DeCelles, P.G., and Giles, K.A., 1996, Foreland basin systems: *Basin Research*, v. 8, p. 105–123, doi: 10.1046/j.1365-2117.1996.01491.x.

DeCelles, P.G., and Hertel, F., 1989, Petrology of fluvial sands from the Amazonian foreland basin, Peru and Bolivia: *Geological Society of America Bulletin*, v. 101, p. 1552–1562, doi: 10.1130/0016-7606(1989)101<1552:POFSFT>2.3.CO;2.

DeCelles, P.G., and Horton, B.K., 2003, Early to middle Tertiary foreland basin development and the history of Andean crustal shortening in Bolivia: *Geological Society of America Bulletin*, v. 115, p. 58–77, doi: 10.1130/0016-7606(2003)115<0058:ETMTFB>2.0.CO;2.

Dewey, J.F., Shackleton, R.M., Chengfa, C., and Yiyin, S., 1988, The tectonic evolution of the Tibetan Plateau: *Philosophical Transactions of the Royal Society of London, ser. A, Mathematical and Physical Sciences*, v. 327, p. 379–413.

Dickinson, W.R., and Suczek, C.A., 1979, Plate tectonics and sandstone compositions: *American Association of Petroleum Geologists Bulletin*, v. 63, p. 2164–2182.

Dorobek, S.L., 1995, Synorogenic carbonate platforms and reefs in foreland basins: Controls on stratigraphic evolution and platform/reef morphology, in Dorobek, S.L., and Ross, G.M., eds., Stratigraphic evolution of foreland basins: Society of Economic Paleontologists and Mineralogists Special Publication 52, 127–148.

Dürr, S.B., 1996, Provenance of Xigaze forearc clastic rocks (Cretaceous, south Tibet): *Geological Society of America Bulletin*, v. 108, p. 669–691, doi: 10.1130/0016-7606(1996)108<0669:POXFAB>2.3.CO;2.

Elliot, T., 1974, Interdistributary bay sequences and their genesis: *Sedimentology*, v. 21, p. 611–622, doi: 10.1111/j.1365-3091.1974.tb01793.x.

England, P.C., and Searle, M., 1986, The Cretaceous-Tertiary deformation of the Lhasa block and its implications for crustal thickening in Tibet: *Tectonics*, v. 5, p. 1–14.

Fielding, E.J., 1996, Tibet uplift and erosion: *Tectonophysics*, v. 260, p. 55–84, doi: 10.1016/0040-1951(96)00076-5.

Guillot, S., Garzanti, E., Baratoux, D., Marquer, D., Maheo, G., and de Sigoyer, J., 2003, Reconstructing the total shortening history of the NW Himalaya: *Geochemistry, Geophysics, Geosystems*, v. 4, doi: 10.1029/2002GC000484.

He, S., 2005, Cretaceous-Tertiary upper crust deformation in southern Tibet [M.S. thesis]: Tucson, University of Arizona, 53 p.

Horton, B.K., and DeCelles, P.G., 2001, Modern and ancient fluvial megafans in the foreland basin system of the central Andes, southern Bolivia: Implications for drainage network evolution in fold-thrust belts: *Basin Research*, v. 13, p. 43–61.

Inden, R.F., and Moore, C.H., 1983, Beach, in Scholle, P.A., Bebout, D.G., and Moore, C.H., eds., Carbonate Depositional Environments: American Association of Petroleum Geologists Memoir 33, p. 211–266.

Ingersoll, R.V., Bullard, T.F., Ford, R.L., Grimm, J.P., Pickle J.D., and Sares, S.W., 1984, The effect of grain size on detrital modes: A test of the Gazi-Dickinson point-counting method: *Journal of Sedimentary Petrology*, v. 54, p. 103–116.

Jones, B., and Desrochers, A., 1992, Shallow platform carbonates, in Walker, R.G., and James, N.P., eds., Facies Models: Response to Sea Level Change: Newfoundland, Canada, Geological Association of Canada, p. 277–301.

Jordan, T.E., 1995, Retroarc foreland basins, in Busby, C., and Ingersoll, R.V., eds., Tectonics of Sedimentary Basins: Cambridge, Massachusetts, Blackwell Scientific, p. 330–362.

Kapp, P., DeCelles, P.G., Leier, A.L., He, S., and Ding, L., 2004, The Gangdese retroarc fold-thrust belt revealed: *Geological Society of America Abstracts with Programs*, v. 36, no. 5, p. 49.

Kidd, W.S.F., Yusheng, P., Chengfa, C., Coward, M.P., Dewey, J.F., Gansser, A., Molnar, P., Shackleton, R.M., and Yiyin, S., 1988, Geological mapping of the 1985 Chinese-British Tibetan (Xizang-Qinghai) Plateau Geotraverse route: *Philosophical Transactions of the Royal Society of London, ser. A, Mathematical and Physical Sciences*, v. 327, p. 287–305.

Kraus, M.J., 1999, Paleosols in clastic sedimentary rocks: Their geologic applications: *Earth-Science Reviews*, v. 47, p. 41–70, doi: 10.1016/S0012-8252(99)00026-4.

Langford, R., and Bracken, B., 1987, Medano Creek Colorado: A model for upper-flow-regime fluvial deposition: *Journal of Sedimentary Petrology*, v. 57, p. 863–870.

Leech, M.L., Singh, S., Jain, A.K., Klemperer, S.L., and Manickavasagam, R.M., 2005, The onset of India-Asia collision: Early, steep subduction required by the timing of UHP metamorphism in the western Himalaya: *Earth and Planetary Science Letters*, v. 234, p. 83–97, doi: 10.1016/j.epsl.2005.02.038.

Leeder, M.R., Smith, A.B., and Jixiang, Y., 1988, Sedimentology, palaeoecology and palaeoenvironmental evolution of the 1985 Lhasa to Golmud Geotraverse: *Philosophical Transactions of the Royal Society of London, ser. A, Mathematical and Physical Sciences*, v. 327, p. 107–143.

Leier, A.L., 2005, The Cretaceous evolution of the Lhasa terrane, southern Tibet [Ph.D. dissertation]: Tucson, University of Arizona, 235 p.

Leier, A.L., Eisenberg, D.A., Kapp, P., and DeCelles, P.G., 2004, Evidence of Cretaceous foreland basins systems in the Lhasa terrane and implications for the tectonic evolution of southern Tibet: *Eos (Transactions, American Geophysical Union)*, v. 85 (47), Fall Meeting Supplement, Abstract T53A–467.

Liu, Z.Q.C., 1988, Geologic map of the Qinghai-Xizang plateau and its neighboring regions: Beijing, Chengdu Institute of Geology and Mineral Resources, Geologic Publishing House, scale: 1:1,500,000.

Mack, G.H., James, W.C., and Monger, H.C., 1993, Classification of paleosols: *Geological Society of America Bulletin*, v. 105, p. 129–136, doi: 10.1130/0016-7606(1993)105<0129:COP>2.3.CO;2.

Miall, A.D., 1978, Facies types and vertical profile models in braided river deposits: A summary, in Miall, A.D., ed., Fluvial Sedimentology: Canadian Society of Petroleum Geologists, Memoir 5, p. 597–604.

Miall, A.D., 1996, The Geology of Fluvial Deposits: Sedimentary Facies, Basin Analysis, and Petroleum Geology: New York, Springer Publishing, 582 p.

Molnar, P., England, P., and Martinod, J., 1993, Mantle dynamics, uplift of the Tibetan Plateau, and the Indian monsoon: *Reviews of Geophysics*, v. 31, p. 357–396, doi: 10.1029/93RG02030.

Murphy, M.A., Yin, A., Harrison, T.M., Dürr, S.B., Chen, Z., Ryerson, F.J., Kidd, W.S.F., Wang, X., and Zhou, X., 1997, Did the Indo-Asian collision alone create the Tibetan Plateau?: *Geology*, v. 25, p. 719–722, doi: 10.1130/0091-7613(1997)025<0719:DTIACA>2.3.CO;2.

Norabuena, E., Leffler-Griffen, L., Mao, A., Dixon, T., Stein, S., Sacks, I.S., Ocola, L., and Ellis, M., 1998, Space geodetic observations of Nazca–South America convergence across the central Andes: *Science*, v. 279, p. 358–362, doi: 10.1126/science.279.5349.358.

Pan, Y., 1993, Unroofing history and structural evolution of the southern Lhasa terrane, Tibetan Plateau: Implications for the continental collision between India and Asia [Ph.D. thesis]: Albany, State University of New York, 287 p.

Raymo, M.E., and Ruddiman, W.F., 1992, Tectonic forcing of late Cenozoic climate: *Nature*, v. 359, p. 117–122, doi: 10.1038/359117a0.

Ratschbacher, L., Frisch, W., Chen, C., and Pan, G., 1993, Deformation and motion along the southern margin of the Lhasa block (Tibet) prior to and during the India-Asia collision: *Journal of Geodynamics*, v. 16, p. 21–54, doi: 10.1016/0264-3707(92)90017-M.

Raymo, M.E., Ruddiman, W.F., and Froelich, P.N., 1988, Influence of late Cenozoic mountain building on ocean geochemical cycles: *Geology*, v. 16, p. 649–653, doi: 10.1130/0091-7613(1988)016<0649:IOLCMB>2.3.CO;2.

Reinson, G.E., 1992, Transgressive barrier island and estuarine systems, in Walker, R.G., and James, N.P., eds., Facies Models: Response to Sea Level Change: Newfoundland, Canada, Geological Association of Canada, p. b179–194.

Şengör, A.M.C., and Natal'in, B.C., 1996, Paleotectonics of Asia: Fragments of a synthesis, in Yin, A., and

- Harrison, T.M., eds., *The Tectonics of Asia*: Cambridge, Cambridge University Press, p. 486–640.
- Shuster, M.W., and Steidtmann, J.R., 1987, Fluvial sandstone architecture and thrust induced subsidence, northern Green River basin, Wyoming, *in* Ethridge, F.G., Flores, R.M., and Harvey, M.D., eds., *Recent Developments in Fluvial Sedimentology*: Society of Economic Paleontologists and Mineralogists Special Publication 39, p. 279–286.
- Smith, A.B., and Xu, J., 1988, Palaeontology of the 1985 Tibet Geotraverse, Lhasa to Golmud: *Philosophical Transactions of the Royal Society of London*, ser. A, *Mathematical and Physical Sciences*, v. 327, p. 53–105.
- Smith, D.G., and Smith, N.D., 1980, Sedimentation in anastomosed river systems: Examples from alluvial valleys near Banff, Alberta: *Journal of Sedimentary Petrology*, v. 50, p. 157–164.
- Tapponnier, P., and 29 others, 1981, The Tibetan side of the India-Eurasia collision: *Nature*, v. 294, p. 405–410.
- Törnqvist, T.E., 1993, Holocene alternation of meandering and anastomosing fluvial systems in the Rhine-Meuse delta (central Netherlands) controlled by sea-level rise and subsoil erodibility: *Journal of Sedimentary Petrology*, v. 63, p. 683–693.
- Tucker, M.E., and Wright, V.P., 1990, *Carbonate Sedimentology*: Cambridge, Massachusetts, Blackwell Scientific, 482 p.
- Walker, R.G., and Harms, J.C., 1971, The Catskill Delta: A prograding muddy shoreline in central Pennsylvania: *The Journal of Geology*, v. 79, p. 381–399.
- Wen, D., Song, B., Iizuka, Y., Ji, J., Chung, S., Liu, D., Yang, H., and Zhang, Q., 2004, Discovery of Late Cretaceous granodiorites with adakitic geochemical signatures from southern Tibet: Petrogenesis and tectonic implications: *Eos (Transactions, American Geophysical Union)*, Fall Meeting Supplement, v. 85, no. 47, Abstract V13B–1465.
- Willis, B., 1993a, Ancient rivers systems in the Himalayan foredeep, Chinji Village area, northern Pakistan: *Sedimentary Geology*, v. 88, p. 1–76, doi: 10.1016/0037-0738(93)90151-T.
- Willis, B., 1993b, Evolution of Miocene fluvial systems in the Himalayan foredeep through a two kilometer-thick succession in northern Pakistan: *Sedimentary Geology*, v. 88, p. 77–121, doi: 10.1016/0037-0738(93)90152-U.
- Yin, A., and Harrison, T.M., 2000, Geologic evolution of the Himalayan-Tibetan orogen: *Annual Review of Earth and Planetary Sciences*, v. 28, p. 211–280, doi: 10.1146/annurev.earth.28.1.211.
- Yin, J., Xu, J., Chengjie, L., and Huan, L., 1988, The Tibetan Plateau: Regional stratigraphic context and previous work: *Philosophical Transactions of the Royal Society of London*, ser. A, *Mathematical and Physical Sciences*, v. 327, p. 5–52.
- Zhang, K.J., 2000, Cretaceous paleogeography of Tibet and adjacent areas (China): Tectonic implications: *Cretaceous Research*, v. 21, p. 23–33, doi: 10.1006/cres.2000.0199.
- Zhang, K.J., Xia, B.D., Wang, G.M., Li, Y.T., and Ye, H.F., 2004, Early Cretaceous stratigraphy, depositional environments, sandstone provenance, and tectonic setting of central Tibet, western China: *Geological Society of America Bulletin*, v. 116, p. 1202–1222, doi: 10.1130/B25388.1.

MANUSCRIPT RECEIVED 19 JANUARY 2006
REVISED MANUSCRIPT RECEIVED 5 MAY 2006
MANUSCRIPT ACCEPTED 18 JULY 2006

Printed in the USA